

The Pennsylvania State University

The J. Jeffrey and Ann Marie Fox Graduate School

**MOVEMENT POTENTIAL OF INFECTIOUS PRIONS BY AMERICAN CROWS
(CORVUS BRACHYRHYNCHOS) IN AN AREA ENDEMIC FOR CHRONIC
WASTING DISEASE**

A Thesis in

Ecology

By

Tyler S. Walters

© 2024 Tyler S. Walters

Submitted in Partial Fulfillment

of the Requirements

for the Degree of

Master of Science

December 2024

The thesis of Tyler S. Walters was reviewed and approved by the following:

W. David Walter

Adjunct Associate Professor of Wildlife Ecology

Thesis Advisor

Frances E. Buderman

Assistant Professor of Quantitative Wildlife Ecology

C. Guilherme Becker

Associate Professor of Biology

Jason P. Kaye

Distinguished Professor of Soil Biogeochemistry

Program Head

ABSTRACT

American crows (*Corvus brachyrhynchos*) can be found throughout much of North America and are known to play a role in the ecology of multiple diseases including West Nile virus (*Orthoflavivirus nilense*), *Campylobacter jejuni*, *Escherichia coli*, *Avipoxvirus*, antibiotic resistant bacteria, and *Collyriclum faba*. Laboratory experiments have also shown the potential for crows to pass infectious prions in their feces after being gavaged with infected meat, however, this has not yet been documented in a wild setting. Collecting fecal and cloacal samples from wild crows for diagnostic purposes and studying the space use and resource selection of crows will contribute to better understanding of their potential role in the movement of infectious prions such as those associated with chronic wasting disease (CWD).

Chronic wasting disease is a transmissible spongiform encephalopathy that is caused by infectious prions and is known to affect cervids such as white-tailed deer (*Odocoileus virginianus*), mule deer (*Odocoileus hemionus*), elk (*Cervus canadensis*), moose (*Alces alces*), red deer (*Cervus elaphus*), and reindeer (*Rangifer tarandus*). Since the discovery of CWD there have been several methods developed to diagnose individuals with the disease. Initially the diagnostic tools available could only be utilized for samples collected postmortem (e.g., retropharyngeal lymph nodes, obex). Continued research and development resulted in the expansion of the available diagnostic tools and the specimen types which can be tested. There were several different early diagnostic tests used to detect the presence of prions and these assays each have their own strengths and weaknesses in terms of cost, time to complete, specificity of results, and level of expertise required to interpret.

Immunohistochemistry (IHC) is one methodology used for the detection of prions that involves fixing thin slices of tissue, treating with an antibody stain that binds to prions, with subsequent viewing under a microscope for interpretation. The IHC does not require amplification, but results can be subjective as they depend on an interpretation by an experienced, certified pathologist. Amplification of the prions within a sample enables the use of additional diagnostic assays. Protein misfolding cyclic amplification (PMCA) increases the concentration of prions within a sample if they are present by

utilizing repeated cycles of protein replication within a substrate and exposure to ultrasound to break down polymers and encourage more replication. Enzyme linked immunosorbent assay (ELISA) involves treatment with proteinase to remove normal prion and then combines the amplified sample material in a solution with monoclonal antibodies. Light absorbency of the solution is measured after a period of incubation to indicate the presence or absence of abnormal prions in the final step of an ELISA. The amplified material can also be tested using western blot which requires sodium dodecyl-sulfate polyacrylamide gel electrophoresis, nitrocellulose sheets, electrophoretic transfer, and treatment with antibodies to produce a radioautograph for interpretation. The IHC, ELISA, and western blot assays that indicate positive results identifies the prions present in a sample are specific to CWD.

These diagnostic tools have been critical in the detection of CWD in wild and captive cervids and surveillance efforts to monitor and understand the geographical spread of the disease. These diagnostic tools are unable to quantify the level of prions present within a sample or their potential disease transmission risk to another individual. Bioassays can be utilized to determine if a given sample and method of exposure result in disease transmission. For a bioassay to be effective the animal receiving the sample must be a species that is naturally susceptible to the infectious agent, or a transgenic animal bred to be susceptible. Mule deer, white-tailed deer, and swine (*Sus domesticus*) are all naturally susceptible. Transgenic mice and Syrian hamsters (*Mesocricetus auratus*) have been bred to be susceptible and are used for bioassays. There are multiple routes of inoculation that have been used in bioassays for CWD, including, but not limited to, intracranial injection, intravenous injection, intraperitoneal injection, aerosolized inoculation, intra-nasal inoculation, and oral inoculation. Although amplified materials are useful for diagnostic purposes, if the goal of a given bioassay is to replicate a natural encounter it is important that the samples being used are a homogenate of non-amplified materials.

There is continued development in the types of samples and protocols that can be used to detect CWD with a focus on antemortem testing option of effected species. In addition, testing samples from species including coyotes (*Canis latrans*), raccoons (*Procyon lotor*), and opossums (*Didelphis*

virginianus) has been conducted because they share the landscape with susceptible species and to investigate their roles in the landscape ecology of infectious prions. We investigated the diagnostic capability of a new method of prion detection, real time quaking induced conversion assays (RT-QuIC), for fecal and cloacal swab samples of wild crows to detect the presence of infectious prions. In total, 61 samples were tested for the presence of infectious prions using RT-QuIC, including both samples from American crows and fish crows (*Corvus ossifragus*). Although reactivity that resulted in increased fluorescent reading was observed for multiple samples using RT-QuIC there was no conclusive evidence that infectious prions were present.

Understanding the way in which crows move across the landscape and their resource selection will also help inform our understanding of the role crows may play. We captured 15 American crows and outfitted them with global positioning system (GPS) transmitters to record locations (n=53,521) along with multiple home range estimators to calculate home range size estimates for individuals by season. We found a high level of variability for 95% home range estimates between individual crows ranging from 0.76 km² to 346.7 km². Covariates representing habitat type, potential resource rich locations, and landscape features were incorporated into integrated step selection functions and Akaike's Information Criteria was used to determine the model of best fit for each individual. The most common model of best fit across individuals and seasons consisted of distance to waste, distance to water, and elevation. We found that some individual crows do interact with captive cervid facilities and carcass dump bins which may result in exposure to infectious materials. Crows were also documented crossing the established regulatory boundaries of disease management areas showing a potential mechanism of infectious material being transferred across these boundaries. The small home range size of most individuals; however, may minimize the likelihood of long distance spread of CWD by crows.

Table of Contents

LIST OF TABLES viii

LIST OF FIGURES..... xi

ACKNOWLEDGEMENTS xvii

Chapter 1 1

 ABSTRACT 2

 INTRODUCTION..... 3

 STUDY AREA..... 5

 METHODS..... 5

 Fecal material 6

 Sample analysis 6

 RESULTS..... 8

 DISCUSSION 9

 RESEARCH IMPLICATIONS..... 11

 REFERENCES..... 13

Chapter 2..... 33

 ABSTRACT 34

 INTRODUCTION..... 35

 STUDY AREA..... 37

 METHODS..... 37

Capture.....	37
Transmitters and banding	38
Estimation of space use and home range size.....	39
Integrated step selection function.....	40
RESULTS.....	42
DISCUSSION	44
RESEARCH IMPLICATIONS.....	45
REFERENCES.....	47

LIST OF TABLES

Table 1.1 Summary of real time quaking induced conversion analysis that resulted in positive chronic wasting disease detections categorized by sample material and species sampled. .. 21

Table 1.2 Summary of bioassay performed with chronic wasting disease prions from an infected species (Species) that resulted in disease transmission identifying sample material of inoculum (Sample material), species inoculated (Bioassay), inoculation method, and source (Reference).
..... 22

Table 1.3 Real time quaking induced conversion assay results from American crow (*Corvus brachyrhynchos*) fecal and cloacal samples collected with a 10⁻³ dilution, including multiple thresholds of detection in Pennsylvania, USA, 2023-2024. 23

Table 1.4 Real time quaking induced conversion assay results from fish crow (*Corvus ossifragus*) fecal and cloacal samples with a 10⁻³ dilution, including multiple thresholds of detection in Pennsylvania, USA, 2023-2024. 24

Table 1.5 Real time quaking induced conversion assay results from opportunistic fecal samples with a 10⁻³ dilution, including multiple runs and multiple thresholds of detection in Pennsylvania, USA, 2023-2024. 25

Table 1.6 Real time quaking induced conversion assay results with total number of wells and proportion of wells that crossed the threshold for American crows (AMCR; *Corvus brachyrhynchos*) and fish crows (FICR; *Corvus ossifragus*) as well as positive and negative controls in Pennsylvania, USA, 2023-2024. 26

Table 2.1 Breeding season home range estimate size for American crows (*Corvus brachyrhynchos*) in Pennsylvania, USA, 2023-2024. Home range estimators were Brownian bridge movement model (BBMM), dynamic Brownian bridge movement model (dBBMM), movement-based kernel density estimation (MKDE) with associated habitat layer, and kernel density estimation with plug-in bandwidth selection (PKDE). 52

Table 2.2 Home range estimate size by season for an American crow (*Corvus brachyrhynchos*) with data for two breeding seasons, a nonbreeding season, and the combined data of all three seasons in Pennsylvania, USA, 2023-2024. Home range estimators were Brownian bridge movement model(BBMM), dynamic Brownian bridge movement model (dBBMM), movement-based kernel density estimation (MKDE) with associated habitat layer, and kernel density estimation with plug-in bandwidth selection (PKDE)..... 54

Table 2.3 Home range estimate size by season for an American crow (*Corvus brachyrhynchos*) with data from one breeding season, one nonbreeding season, and the combined data of these seasons in Pennsylvania, USA, 2023-2024. Home range estimators were Brownian bridge movement model (BBMM), dynamic Brownian bridge movement model (dBBMM), movement-based kernel density estimation (MKDE) with associated habitat layer, and kernel density estimation with plug-in bandwidth selection (PKDE). 55

Table 2.4 Minimum, maximum, and average American crow (*Corvus brachyrhynchos*) home range estimates for breeding and nonbreeding seasons in Pennsylvania, USA, 2023-2024. Home range estimators were Brownian bridge movement model (BBMM), dynamic Brownian bridge model (dBBMM), movement-based kernel density estimation (MKDE) with associated habitat layer, and kernel density estimation with plug-in bandwidth selection (PKDE). 56

Table 2.5 Integrated step selection function model of best fit for individual American crows (*Corvus brachyrhynchos*) during the breeding season with coefficient, exponential coefficient, and upper and lower 95% confidence intervals (CI) for each model element. Pennsylvania, USA, 2023. 57

Table 2.6 Integrated step selection function model of best fit for individuals with multiple seasons of data collected with the coefficient, exponential coefficient, and upper and lower 95% confidence intervals (CI) for each model element. Pennsylvania, USA, 2023-2024. 59

Table 2.7 Integrated step selection functions models for American crows (*Corvus brachyrhynchos*) for each season (Breeding, Nonbreeding, Combined) in Pennsylvania, USA, 2023-2024 using Akaike information criterion (AICc). Number of parameters in the model (K), change in corrected Akaike information criterion from the lowest AICc ($\Delta AICc$), and AICc model weights ($AICc\omega$) were used to determine top model and strength of competing models. Covariates included: distance to the nearest water (water), distance to nearest forest (forest), distance to open (open), distance to nearest human population of 2500 people per square mile (h_pop), distance to nearest landfill or compost facility (waste), distance to the nearest carcass disposal dumpster or positive captive facility (risk), distance to the nearest primary or secondary road (road), and elevation in meters (elevation). All models also incorporated step length as a model element. 60

LIST OF FIGURES

Figure 1.1 Real-time quaking-induced conversion assay results from American crow (*Corvus brachyrhynchos*) fecal samples in Pennsylvania, USA, 2023-2024. For each individual 18 replicate wells were tested and the number of wells that exceeded the fluorescence threshold is represented in blue and the wells that did not exceed the threshold are represented in gray. A) 5X threshold; B) 10X threshold. 27

Figure 1.2 Real-time quaking-induced conversion assay results from American crow (*Corvus brachyrhynchos*) cloacal samples in Pennsylvania, USA, 2023-2024. For each individual 18 replicate wells were tested and the number of wells that exceeded the fluorescence threshold is represented in green and the wells that did not exceed the threshold are represented in gray. A) 5X threshold; B) 10X threshold. 28

Figure 1.3 Real-time quaking-induced conversion assay results from fish crow (*Corvus ossifragus*) fecal and cloacal samples in Pennsylvania, USA, 2023-2024. For each sample 18 replicate wells were tested and the number of wells that exceeded the fluorescence threshold is represented in purple for fecal samples and dark blue for cloacal samples, the wells that did not exceed the threshold are represented in gray. A) 5X threshold; B) 10X threshold. 29

Figure 1.4 Fluorescence of real-time quaking-induced conversion assay for samples of American crow (*Corvus brachyrhynchos*) feces (blue) in Pennsylvania, USA, 2023-2024, with positive controls (red), and negative controls (yellow). Threshold values are included for the 5X threshold (gray), and 10X threshold (black) A) The fluorescence values including the maximum values for these sample wells; B) A focused view of the sample well fluorescence in relation to the threshold values. 30

Figure 1.5 Fluorescence of real-time quaking-induced conversion assay for samples of American crow (*Corvus brachyrhynchos*) cloacal swabs (green) in Pennsylvania, USA, 2023-2024, with positive controls (red), and negative controls (yellow). Threshold values are included for the 5X threshold (gray), and 10X threshold (black) A) The fluorescence values including the maximum values for these sample wells. B) A focused view of the sample well fluorescence in relation to the threshold values..... 31

Figure 1.6 Fluorescence of real-time quaking-induced conversion assay for samples of fish crow (*Corvus ossifragus*) feces (purple) and cloacal swabs (dark blue) in Pennsylvania, USA, 2023-2024, with positive controls (red), and negative controls (yellow). Threshold values are included for the 5X threshold (gray), and 10X threshold (black) A) The fluorescence values including the maximum values for these sample wells. B) A focused view of the sample well fluorescence in relation to the threshold values. 32

Figure 2.1 A) Breeding season GPS locations for AMCR001 in Pennsylvania, USA, 2023. Estimators of home range included: B) Brownian bridge movement model, C) dynamic Brownian bridge movement model, D) movement-based kernel density with null habitat, E) movement-based kernel density estimator with 4 land cover categories (water, developed, forest, open), F) movement-based kernel density with elevation, G) kernel density estimator with plug-in bandwidth selection. Isopleths are 50% (red), 80% (orange), 90% (yellow), and 95%(green). 62

Figure 2.2 A) Breeding season GPS locations for AMCR002 in Pennsylvania, USA, 2023.

Estimators of home range included: B) Brownian bridge movement model, C) dynamic Brownian bridge movement model, D) movement-based kernel density with null habitat, E) movement-based kernel density estimator with 4 land cover categories (water, developed, forest, open), F) movement-based kernel density with elevation, G) kernel density estimator with plug-in bandwidth selection. Isopleths are 50% (red), 80% (orange), 90% (yellow), and 95%(green). 63

Figure 2.3 A) Breeding season GPS locations for AMCR007 in Pennsylvania, USA, 2023.

Estimators of home range included: B) Brownian bridge movement model, C) dynamic Brownian bridge movement model, D) movement-based kernel density with null habitat, E) movement-based kernel density estimator with 4 land cover categories (water, developed, forest, open), F) movement-based kernel density with elevation, G) kernel density estimator with plug-in bandwidth selection. Isopleths are 50% (red), 80% (orange), 90% (yellow), and 95%(green). 64

Figure 2.4 A) Nonbreeding season GPS locations for AMCR007 in Pennsylvania, USA, 2023-2024.

Estimators of home range included: B) Brownian bridge movement model, C) dynamic Brownian bridge movement model, D) movement-based kernel density with null habitat, E) movement-based kernel density estimator with 4 land cover categories (water, developed, forest, open), F) movement-based kernel density with elevation, G) kernel density estimator with plug-in bandwidth selection. Isopleths are 50% (red), 80% (orange), 90% (yellow), and 95%(green). 65

Figure 2.5 A) Breeding season GPS locations for AMCR007 in Pennsylvania, USA, 2024.

Estimators of home range included: B) Brownian bridge movement model, C) dynamic Brownian bridge movement model, D) movement-based kernel density with null habitat, E) movement-based kernel density estimator with 4 land cover categories (water, developed, forest, open), F) movement-based kernel density with elevation, G) kernel density estimator with plug-in bandwidth selection. Isopleths are 50% (red), 80% (orange), 90% (yellow), and 95%(green). 66

Figure 2.6 A) All season combined GPS locations for AMCR007 in Pennsylvania, USA, 2023-2024.

Estimators of home range included: B) Brownian bridge movement model, C) dynamic Brownian bridge movement model, D) movement-based kernel density with null habitat, E) movement-based kernel density estimator with 4 land cover categories (water, developed, forest, open), F) movement-based kernel density with elevation, G) kernel density estimator with plug-in bandwidth selection. Isopleths are 50% (red), 80% (orange), 90% (yellow), and 95%(green). 67

Figure 2.7 A) Nonbreeding season GPS locations for AMCR011 in Pennsylvania, USA, 2023-2024.

Estimators of home range included: B) Brownian bridge movement model, C) dynamic Brownian bridge movement model, D) movement-based kernel density with null habitat, E) movement-based kernel density estimator with 4 land cover categories (water, developed, forest, open), F) movement-based kernel density with elevation, G) kernel density estimator with plug-in bandwidth selection. Isopleths are 50% (red), 80% (orange), 90% (yellow), and 95%(green). 68

Figure 2.8 A) Breeding season GPS locations for AMCR011 in Pennsylvania, USA, 2024.

Estimators of home range included: B) Brownian bridge movement model, C) dynamic Brownian bridge movement model, D) movement-based kernel density with null habitat, E) movement-based kernel density estimator with 4 land cover categories (water, developed, forest, open), F) movement-based kernel density with elevation, G) kernel density estimator with plug-in bandwidth selection. Isopleths are 50% (red), 80% (orange), 90% (yellow), and 95%(green). 69

Figure 2.9 A) All seasons combined GPS locations for AMCR011 in Pennsylvania, USA, 2023-2024.

Estimators of home range included: B) Brownian bridge movement model, C) dynamic Brownian bridge movement model, D) movement-based kernel density with null habitat, E) movement-based kernel density estimator with 4 land cover categories (water, developed, forest, open), F) movement-based kernel density with elevation, G) kernel density estimator with plug-in bandwidth selection. Isopleths are 50% (red), 80% (orange), 90% (yellow), and 95%(green). 70

Figure 2.10 A) Breeding season GPS locations for AMCR012 in Pennsylvania, USA, 2024.

Estimators of home range included: B) Brownian bridge movement model, C) dynamic Brownian bridge movement model, D) movement-based kernel density with null habitat, E) movement-based kernel density estimator with 4 land cover categories (water, developed, forest, open), F) movement-based kernel density with elevation, G) kernel density estimator with plug-in bandwidth selection. Isopleths are 50% (red), 80% (orange), 90% (yellow), and 95%(green). 71

Figure 2.11 A) Breeding season GPS locations for AMCR013 in Pennsylvania, USA, 2024.

Estimators of home range included: B) Brownian bridge movement model, C) dynamic Brownian bridge movement model, D) movement-based kernel density with null habitat, E) movement-based kernel density estimator with 4 land cover categories (water, developed, forest, open), F) movement-based kernel density with elevation, G) kernel density estimator with plug-in bandwidth selection. Isopleths are 50% (red), 80% (orange), 90% (yellow), and 95%(green). 72

Figure 2.12 A) Breeding season GPS locations for AMCR014 in Pennsylvania, USA, 2024.

Estimators of home range included: B) Brownian bridge movement model, C) dynamic Brownian bridge movement model, D) movement-based kernel density with null habitat, E) movement-based kernel density estimator with 4 land cover categories (water, developed, forest, open), F) movement-based kernel density with elevation, G) kernel density estimator with plug-in bandwidth selection. Isopleths are 50% (red), 80% (orange), 90% (yellow), and 95%(green). 73

Figure 2.13 A) Breeding season GPS locations for AMCR015 in Pennsylvania, USA, 2024.

Estimators of home range presented include: B) Brownian bridge movement model, C) dynamic Brownian bridge movement model, D) movement-based kernel density with null habitat, E) movement-based kernel density estimator with 4 land cover categories (water, developed, forest, open), F) movement-based kernel density with elevation, G) kernel density estimator with plug-in bandwidth selection. Isopleths are 50% (red), 80% (orange), 90% (yellow), and 95%(green). 74

ACKNOWLEDGEMENTS

This document is the culmination of the hard work, patience, knowledge, blood, sweat, and tears of many people who I can only hope know how grateful I am. First, I would like to thank my advisor David Walter, working with crows was more challenging than we ever anticipated and in addition to his knowledge and guidance his immense patience and belief in me empowered me to find success. Gui Becker and Franny Buderman, members of my committee, shared their expertise and offered perspectives that helped shape this research and helped me grow as a scientist, for which I am very thankful.

This project would not have been possible without the funding and support of the U.S. Department of Agriculture-Animal Plant and Health Inspection Service-Wildlife Services at the National Wildlife Research Center along with the ongoing work of Kurt VerCauteren. Any opinions, findings, conclusions, or recommendations expressed in this publication are those of the authors and should not be construed to represent any official USDA or U.S. Government determination or policy. I am thankful for the partnerships with the PA Game Commission and University of Pennsylvania's Wildlife Futures Program that were essential to the success of this project. Dave Pearce, Alberto Fameli, Jessie Edson, Alberto Cruz, Kyle Smelter, Karter Witmer, and Kevin Lamp not only endured hours of hearing me talk about crows but also days in a truck or blind in pursuit of the elusive crow capture and are owed many thanks.

My parents, Anne and Steve Walters, have given me the belief and the freedom necessary to pursue my passions and their continued support has made this achievement possible. My older brother R.J. has been an invaluable lifelong mentor to me and experiencing crow capture together is a memory of lifetime. Jennifer Hoy-Petersen has worn many hats as lab analyst, crow capture assistant, and life partner. I cannot adequately express my gratitude for the daily love and support she has shown me. A special thanks goes out to the doctors and nurses of St. Luke's Hospital whose skilled care made it possible for me to be here after an accident on September 19, 2019, changed the trajectory of my life. Last but not least I would like to thank the crows.

Chapter 1

Chronic wasting disease prion shedding potential of American crows and fish crows.

Chapter 1 was written in collaboration with Jennifer Hoy-Petersen, Erick Gagne, Michelle Gibison, Kurt C. VerCauteren, and W. David Walter. I have included this manuscript on the following pages as formatted for the Journal of Wildlife Management.

ABSTRACT

Chronic wasting disease (CWD) is a transmissible spongiform encephalopathy that is caused by infectious prions. Chronic wasting disease is known to affect cervids such as white-tailed deer (*Odocoileus virginianus*), mule deer (*Odocoileus hemionus*), elk (*Cervus canadensis*), moose (*Alces alces*), red deer (*Cervus elaphus*), and reindeer (*Rangifer tarandus*). Detection of the disease is crucial to furthering our understanding of its ecology and to inform management decisions. Initially, detection methods were limited to postmortem samples from a select few tissues including lymph nodes and obex. Real-time quaking-induced conversion (RT-QuIC) has emerged as a reliable time and resource efficient assay for prion detection. American crows (*Corvus brachyrhynchos*) have been shown in a lab setting to have the potential to pass infectious prions in their feces after being gavaged with infected meat. We developed a crow specific RT-QuIC assay and utilized it to test 61 fecal and cloacal swabs from wild American crows and fish crows (*Corvus ossifragus*). The presence of infectious prions has not previously been documented in wild crows. Although reactivity that resulted in increased fluorescent reading was observed for multiple samples likely from infectious prions, RT-QuIC does not provide conclusive evidence that infectious prions from CWD were present. Further testing of these samples with alternate assays would improve our understanding of the infectious prions present in samples collected from crows in our study area where CWD is endemic.

KEYWORDS American crows, chronic wasting disease, *Corvus brachyrhynchos*, *Corvus ossifragus*, CWD, fish crows, Pennsylvania, RT-QuIC

INTRODUCTION

Prion diseases are a suite of fatal neurodegenerative diseases caused by modifications to the prion protein (PrP; Prusiner 1998). Prusiner (1998) coined the term prion as an aggregation of the terms proteinaceous and infectious after discovering that prion diseases are not caused by a known pathogen such as a virus or bacteria, but rather by proteinaceous infectious particles. Chronic wasting disease (CWD), scrapie, bovine spongiform encephalopathy, Creutzfeldt-Jakob disease, and variant Creutzfeldt-Jakob disease are all examples of prion diseases. Gough and Maddison (2010) compiled a review of prion disease transmission including examples of infectious prion detection in feces, urine, saliva, nasal secretions, milk, placenta, and skin. Not all prion diseases are capable of being spread through these categories of materials; however, CWD can spread effectively through both horizontal and environmental transmission (Gilch et al. 2011). Chronic wasting disease is a transmissible spongiform encephalopathy that was first detected in mule deer (*Odocoileus hemionus*) in a captive wildlife facility in Colorado in 1967 (Williams and Young 1980). Since its discovery it has been determined that a variety of cervid species including white-tailed deer (*Odocoileus virginianus*), mule deer, elk (*Cervus canadensis*), moose (*Alces alces*), red deer (*Cervus elaphus*), and reindeer (*Rangifer tarandus*) are susceptible to CWD. In addition to North America, CWD has been detected in South Korea, Finland, Sweden, and Norway (Ågren et al. 2021; Benestad et al. 2016; Finnish Food Safety Authority Evira 2018; Sohn et al. 2002).

To effectively model CWD transmission and make informed management decisions, understanding the dynamics of CWD transmission is integral. One facet of these dynamics is identifying which animal species are capable of shedding infectious prions in the environment. The infectious prions that cause CWD in cervid species can be found in the feces, urine, saliva, and carcasses of infected individuals (Haley et al. 2011; Henderson et al. 2017; Pulford et al. 2012; Safar et al. 2008; Tamguney et al. 2009, 2012). Infectious prions may also be found in soil (Miller et al. 2004), water (Nichols et al. 2009), and in shared resources such as mineral licks (Plummer et al. 2018). Another facet is to identify

which sample materials where CWD prions have been found to be present pose a risk for disease spread to individuals exposed to those samples (Table 1.1).

There are a variety of different scavenger species that may come in contact with infectious materials and American crows (*Corvus brachyrhynchos*) have been documented to be a frequent scavenger of deer carcasses (Prior and Weatherhead 1991). American crows gavaged with tissue containing infectious scrapie prions subsequently shed infectious prions in their feces within a controlled laboratory setting (VerCauteren et al. 2012). Using a mouse bioassay, mice inoculated with feces from these crows developed the associated prion disease (VerCauteren et al. 2012). The impetus for our project was to build upon these previous findings and investigate the possible presence of infectious CWD prions in samples collected from wild crows interacting naturally with their environment in an area endemic for CWD.

The United States Department of Agriculture (USDA) has approved both immunohistochemistry (IHC) and enzyme-linked immunosorbent assay (ELISA) of medial retropharyngeal lymph nodes and obex as diagnostic tests for official postmortem testing in cervids (USDA 2024). Antemortem detection of CWD has been done using mouse bioassays (Fischer et al. 2013; Haley et al. 2009), protein-misfolding cyclic amplification (Kurt et al. 2007; Pulford et al. 2012), and real-time quaking-induced conversion (RT-QuIC) (Henderson et al. 2013, 2017; Tewari et al. 2021, 2022). The RT-QuIC assay is a highly sensitive assay for prion detection that has been applied to a variety of species and sample materials (Table 1.2).

The benefit of RT-QuIC is that it combines the amplification and diagnostic elements of prion detection into a single time and cost-efficient process. Real time quaking induced assays detect the presence of prions through the fluorescence of an introduced dye that binds to misfolded proteins which are amplified in a substrate through regulated cycles of shaking and rest (Atarashi et al. 2011). Some advantages of this testing methodology are that it does not require maintaining a colony of live animals, takes only days to run, and does not rely on the trained eye of a specialized pathologist. A unique assay

protocol must be developed for each new species and sample type tested using RT-QuIC. Therefore, our first objective was to develop a protocol for an assay for cloacal and fecal samples from American crows and fish crows (*Corvus ossifragus*). Given the previous lab work pertaining to the ability of crows to pass infectious prions in feces we expect these samples from wild crows to be viable samples and result in increased fluorescence in RT-QuIC assays if infectious prions are present. The frequency of crows coming into contact with infectious prions and the amount of exposure required for detectability are unknown and as such it may take a large sample size to capture any detections even if this process is occurring on the landscape. Our objective is to use RT-QuIC to test samples from wild crows to investigate if there is any initial indication of the presence of infectious prions. Any initial detections in our study will be the first documentation of prions in samples from wild crows. Reactivity in the newly developed RT-QuIC assays indicates the presence of prions in the sample but does not indicate the specific type of prion and detections found as a part of our study will establish the need for future research utilizing other more time and resource intensive assays to determine if the reactivity is due to the presence of CWD.

STUDY AREA

Our study area was in central Pennsylvania, USA, in Blair, Bedford, Cambria, Franklin, Fulton, Huntingdon, Lancaster, and Somerset counties. We concentrated our study area within Disease Management Area 2 (DMA 2) created by the Pennsylvania Game Commission (PGC) in response to detection of CWD in wild and captive deer in 2012 that has expanded in subsequent years due to additional detections of positive wild deer (Pennsylvania Game Commission 2020)

METHODS

This work was approved by the Pennsylvania State University Institutional Animal Care and Use Committee and authorized through permit PROTO202102055. All bird capture was done in accordance with the federal Bird Banding Laboratory guidelines and authorized through permit 08660 and 08860-AB.

Fecal material

We obtained cloacal swabs from individual captured crows by inserting rayon tipped swabs (Puritan Medical Products, Guilford, Maine, USA) into the cloaca and moving the swab in a circular motion 2-4 times with gentle pressure. In addition, fecal swabs were collected when available. Birds were held individually in cloth capture bags prior to processing and swabs were taken of any fecal material the individual deposited in the bag, and any fecal material expressed during the handling of the bird. To increase the sample size of fecal samples, plastic sheeting was placed at known perching locations of crows and swabs were taken of fecal material deposited on this sheeting. Similar methods have been used across Europe and North America to sample for disease presence in avian feces (Oravcova et al. 2013, 2014). Motion activated trail cameras (PRADCO Outdoor Brands, Birmingham, Alabama) were used to monitor these sample locations to confirm the presence of crows. It is possible that in addition to crow feces, these samples may also contain some material from other bird species using the same area such as: common raven (*Corvus corax*), American robin (*Turdus migratorius*), turkey vulture (*Cathartes aura*), black vulture (*Coragyps atratus*), and European starling (*Sturnus vulgaris*). Samples were stored at -80°C following collection until their analysis.

Sample analysis

Fecal material was collected from captive American crows in a rehab facility to use as a negative baseline for calibrating the diagnostic assay. Lymph nodes from white-tailed deer with known CWD status were used as positive and negative controls as well as for spiking the fecal material of captive crows. These spiked samples were used as a proxy for fecal material from crows with a known presence or absence of CWD prions for the development and calibration of our new assay protocol. These lymph nodes were confirmed as positive or negative by enzyme-linked immunosorbent assay and immunohistochemistry following the U.S. Department of Agriculture approved protocols in the accredited Veterinary Diagnostic Laboratory at the University of Pennsylvania's Wildlife Futures Program (WFP). Each fecal and cloacal swab was thawed before adding 400ul of 1x phosphate buffered saline (1XPBS) and pulse-vortexed for

30 seconds before removing the swab and brief centrifugation. Supernatant was extracted and diluted to 10^{-3} using commercially available dilution buffer (CWD 10X Sample Dilution Buffer, VMRD, Pullman, Washington, USA) containing 0.1% SDS and 1XPBS. The reaction solution for RT-QuIC was prepared using commercially available AA-90-231 Syrian Hamster substrate (0.1mg/mL, CWD Amplification Reagent VMRD) and reaction solution (CWD 5X Reaction Buffer, VMRD) containing 5XPBS pH 7.4, 0.85M NaCl, 5mM EDTA, and 50 μ l Thioflavin T (ThT). Each well of a 96-well optical-bottom plate (Item no: 655096, Greiner Bio-One, Monroe, North Carolina, USA) was filled with 98 μ l reaction solution and 2 μ l of either diluted crow sample or control. The positive and negative control were added to 3 wells each, and the crow samples were added to 6 wells each. The assay was conducted at WFP using the BMG FLUOstar plate reader (BMG Labtech, Offenburg, Germany) for 62 hours using the following settings: 44°C, 250 cycles (700RPM with 60s shake/60s rest cycles), fluorescent scans every 15 minutes, at a gain of 1350 relative fluorescence units. Two threshold values were calculated, which have been used previously for RT-QuIC analysis, by averaging the fluorescence values from the first three cycle scans and adding 5X or 10X the standard deviation of these fluorescence values (Henderson et al. 2015a; Haley et al. 2020). From here forward these thresholds will be referred to as the 5X threshold or 10X threshold and in reference to if the fluorescence of a specific sample well exceeded these thresholds. When viewing the fluorescence graph of an RT-QuIC assay it is expected to see a lag phase, a growth phase, and a plateau phase that cross the 5X and 10X thresholds for wells in which an interaction is occurring. A sample well that exceeded these thresholds was considered to have an interaction occurring that is beyond that expected from a neutral well or from auto conversion of the substrate.

The positive control of a well plate was considered positive if at least two of three wells crossed the threshold, and the negative control was considered negative if at least two of three wells did not cross the threshold. If the positive or negative control failed to meet these parameters, the data from the associated well plate was considered invalid.

RESULTS

In total 61 samples were tested for the presence of CWD prions with RT-QuIC. These samples were given individual identifiers consisting of the four-letter species code (AMCR, FICR), an individual bird identifier (001-023), and the sample material (fecal, cloacal). Opportunistic fecal samples were identified as “FS” followed by an individual identifier (001-009). For each sample, 3 runs of 6 wells were completed resulting in 18 total wells analyzed for each sample. A total of 1098 wells of the samples from American crows, fish crows, and opportunistic samples were run with an additional 42 wells of positive control lymph nodes and 42 wells of negative control (3 wells of each in every well plate). One well of negative control from a single plate was excluded due to high initial fluorescence that exceeded the 5x threshold from the initiation of the run.

Of the 26 samples from American crows, 18 samples had at least one well exceed the 5X threshold (Figure 1.1; Figure 1.2). All 18 wells of AMCR005 fecal sample, AMCR014 fecal sample one, and AMCR014 fecal sample two exceeded the 5X threshold (Table 1.3). For samples from fish crows, 19 of 26 had at least one well that exceeded the threshold (Figure 1.3), including all 18 wells of FICR004 cloacal sample, FICR014 cloacal sample, and FICR021 fecal sample (Table 1.4). The opportunistic fecal samples had seven of nine samples with at least one well exceeding the threshold including three samples that had all 18 wells cross the threshold.

For the higher 10X threshold, 12 American crow samples had at least one well that exceeded the threshold (Figure 1.1; Figure 1.2). Sample AMCR005 fecal had 8 out of 18 wells with a level of fluorescence above the 10X threshold which was the most of any American crow (Table 1.3). For fish crows, 16 of 26 samples had at least one well exceed the 10X threshold (Figure 1.3). Sample FICR014 cloacal had all 18 wells exceed the 10X threshold which was the most of any fish crow (Table 1.4). Additionally, seven of nine opportunistic fecal samples had at least one well exceed the 10X threshold (Table 1.5).

Fecal samples from fish crows had the highest proportion of wells exceed the threshold with 40/54 (74.07%) exceeding the 5X threshold and 24/54 (44.44%) exceeding the 10X threshold. The lowest proportion of wells that exceeded the threshold resulted from the cloacal samples of American crows with 37/252 (14.68%) exceeding the 5X threshold and 9/252 (3.57%) exceeding the 10X threshold. Overall, fecal samples had a higher proportion of wells exceed the threshold with 192/432 (44.44%) exceeding the 5X threshold and 79/432 (18.29%) exceeding the 10X threshold compared to cloacal samples having 159/666 (23.87%) exceed the 5X threshold and 79/666 (11.86%) exceed the 10X threshold. When aggregated by species the fish crows had a higher proportion of wells exceed the threshold with 162/468 (34.62%) exceeding the 5x threshold and 94/468 (20.09%) exceeding the 10X threshold compared to American crows which had 130/468 (27.78%) exceed the 5x threshold and 35/468 (7.48%) exceed the 10X threshold.

Across all runs 42/42 (100%) of positive control wells exceeded both the 5X and 10X thresholds (Table 1.6). In relation to the 5X threshold 7/41(17.07%) of negative control wells exceeded the threshold, and 3/41 (7.32%) of negative control wells exceeded the 10X threshold. These wells show that possible auto conversion of the substrate and variation between wells can result in a small proportion of wells exceeding the thresholds in contradiction to the true status of the sample contents. Cloacal samples from American crows had a lower percentage of wells that exceeded the threshold than that of the negative controls for 37/252 (14.68%) and 9/252 (3.57%) for 5x and 10x thresholds, respectively. All other aggregation of samples by either species, sample material, or both resulted in a higher proportion of wells that exceeded the fluorescence thresholds than that of the negative controls.

DISCUSSION

When viewing the fluorescence graph of an RT-QuIC assay it is expected to see a lag phase, a growth phase, and a plateau phase that crosses the 5X and 10X thresholds for wells in which an interaction is occurring. To illustrate this, we selected wells from three well plates that, as a group, contain wells of each of the four sample types (American crow cloacal, American crow fecal, fish crow cloacal, and fish

crow fecal) crossing the thresholds (Figure 1.4; Figure 1.5; Figure 1.6). There is variation amongst the wells that cross the thresholds with some closely resembling or exceeding the positive control and others resulting in less prominent curves of increased fluorescence. It is important to remember that the positive control is deer lymph nodes, and it is unknown how a positive control crow fecal sample may differ. Time is another important factor to consider when interpreting RT-QuIC because the longer a run goes the higher likelihood of auto conversion of the substrate occurring. Although the fecal samples from American crows do not reach as high of maximum fluorescence as the other sample types, they do show a pattern of exceeding the thresholds in a shorter amount of time (Figure 1.4).

We observed indications that there is some biological or chemical process that is causing an increase in fluorescence in some sample wells. There is inconsistency across samples, individual wells, and runs that were not consistent with the pattern of results seen from validated RT-QuIC protocols such as that for lymph nodes. Since this is the first usage of RT-QuIC on fecal material from crows and given these results, the causative agent cannot be determined by RT-QuIC alone. It is imperative that the results be confirmed by additional diagnostic assays to ensure that there is not an interaction between the reagents, substrate, and crow fecal material that may create false positives or negatives from RT-QuIC. Although the presence or absence of CWD prions within a sample cannot be determined, the clear indication that some interaction between samples and substrate is occurring supports the importance of continued analyses of these samples. Next steps would include using the more time and resource intense western blot or protein misfolding cyclic amplification as they can be calibrated to specifically identify the presence of CWD prions.

When developing an RT-QuIC assay for a new species or sample type it would be ideal to have examples of these samples with known status confirmed through other diagnostic assays to use as a control to determine the appropriate protocol. American crows and fish crows have not previously had CWD prion detection using any diagnostic assays, so an approximation was needed to develop the testing protocol. This was achieved through the spiking of known negative feces from captive crows with lymph

nodes from white-tailed deer that have a confirmed positive or negative status. This approximation allows for the development of a preliminary RT-QuIC assay. We included a 5x standard deviation threshold and a 10x standard deviation threshold in our analysis as both have been used in previous RT-QuIC research (Henderson et al. 2015a; Haley et al. 2020). The 5X threshold had more negative controls exceed it than the 10X threshold and visually some of the wells that exceeded the 5X threshold but did not exceed the 10X threshold did not display the growth curve that would be expected with prion presence. The RT-QuIC protocol we developed can be further refined once a confirmed positive Corvidae fecal sample is available, wild or captive, to use to calibrate the temperature, time, concentration, and threshold more accurately. If this refinement to the RT-QuIC protocol has a high level of specificity and sensitivity, then it can be used as a diagnostic assay for future crow fecal testing.

RESEARCH IMPLICATIONS

We developed an initial protocol for determining presence of prions in fecal and cloacal samples from crows using RT-QuIC which can be used for continued testing. The reactivity observed in various sample types from an area where CWD has been present for over a decade supports the hypothesis that crows may ingest infectious prions and demonstrates the need for further research on crows and other avian species. The knowledge of how wild avian species contribute to the spread of infectious prions is important to the process of making informed, specific, and effective management decisions related to both wild and captive cervids.

ACKNOWLEDGEMENTS

The U.S. Department of Agriculture-Animal Plant and Health Inspection Service-Wildlife Services provided funding for this research. The Pennsylvania Game Commission provided specific information regarding CWD within our study area and provided access to locations for crow capture. Margaret Brittingham provided her invaluable expertise as a master bander for this project. This project would not have been possible without the following individuals who devoted many hours to assist with crow

capture: D. Pearce, A. Fameli, J. Edson, A. Cruz, K. Smelter, K. Witmer, E. Miller, J. Yacabucci, K. Lamp, and R. Walters. Any opinions, findings, conclusions, or recommendations expressed in this publication are those of the authors and should not be construed to represent any official USDA or U.S. Government determination or policy. Any use of trade, firm, or product names is for descriptive purposes only and does not imply endorsement by the U.S. Government.

REFERENCES

- Ågren, E. O., K. Sörén, D. Gavier-Widén, S. L. Benestad, L. Tran, K. Wall, G. Averhed, N. Doose, J. Våge, and M. Nöremark. 2021. First detection of chronic wasting disease in moose (*Alces alces*) in Sweden. *Journal of wildlife diseases* 57(2):461–463.
- Angers, R. C., T. S. Seward, D. Napier, M. Green, E. Hoover, T. Spraker, K. O'rourke, A. Balachandran, and G. C. Telling. 2009. Chronic wasting disease prions in elk antler velvet. *Emerging Infectious Diseases* 15(5):696–703.
- Atarashi, R., K. Sano, K. Satoh, and N. Nishida. 2011. Real-time quaking-induced conversion a highly sensitive assay for prion detection . *Prion* 5(3):150–153.
- Benestad, S. L., G. Mitchell, M. Simmons, B. Ytrehus, and T. Vikøren. 2016. First case of chronic wasting disease in Europe in a Norwegian free-ranging reindeer. *Veterinary Research* 47(1):88.
- Browning, S. R., G. L. Mason, T. Seward, M. Green, G. a. J. Eliason, C. Mathiason, M. W. Miller, E. S. Williams, E. Hoover, and G. C. Telling. 2004. Transmission of prions from mule deer and elk with chronic wasting disease to transgenic mice expressing cervid PrP. *Journal of Virology* 78(23): 13345–13350.
- Cheng, Y. C., S. Hannaoui, T. R. John, S. Dudas, S. Czub, and S. Gilch. 2016. Early and non-invasive detection of chronic wasting disease prions in elk feces by real time quaking induced conversion . *PLoS One* 11(11): e0166187.
- Cheng, Y. C., S. Hannaoui, T. R. John, S. Dudas, S. Czub, and S. Gilch. 2017. Real-time quaking-induced conversion assay for detection of cwd prions in fecal material *Journal of Visualized Experiments* 127:e56373.
- Cooper, S. K., C. E. Hoover, D. M. Henderson, N. J. Haley, C. K. Mathiason, and E. A. Hoover. 2019. Detection of CWD in cervids by RT-QuIC assay of third eyelids . *PLoS One* 14(8):e0221654.
- Denkers, N. D., D. M. Seelig, G. C. Telling, and E. A. Hoover. 2010. Aerosol and nasal transmission of chronic wasting disease in cervidized mice. *Journal of General Virology*, 91(6):1651–1658.

- Elder, A. M., D. M. Henderson, A. V. Nalls, E. A. Hoover, A. E. Kincaid, J. C. Bartz, and C. K. Mathiason. 2015. Immediate and ongoing detection of prions in the blood of hamsters and deer following oral, nasal, or blood inoculations . *Journal of Virology* 89(14):7421–7424.
- Elder, A. M., D. M. Henderson, A. V. Nalls, J. M. Wilham, B. W. Caughey, E. A. Hoover, A. E. Kincaid, J. C. Bartz, and C. K. Mathiason. 2013. *In Vitro* detection of prionemia in TSE-infected cervids and hamsters . *PLoS One* 8(11):e80203.
- Finnish Food Safety Authority Evira. 2018. Moose found dead in forest with chronic wasting disease. <<https://valtioneuvosto.fi/en/-/1410837/evira-metsaan-kuolleella-hirvella-naivetystauti>>. Accessed 30 Oct 2024.
- Ferreira, N. C., J. M. Charco, J. Plagenz, C. D. Orru, N. D. Denkers, M. A. Metrick, A. G. Hughson, K. A. Griffin, B. Race, E. A. Hoover et al.. 2021. Detection of chronic wasting disease in mule and white-tailed deer by RT-QuIC analysis of outer ear. *Scientific Reports* 11(1):7702.
- Fischer, J. W., T. A. Nichols, G. E. Phillips, and K. C. Vercauteren. 2013. Procedures for identifying infectious prions after passage through the digestive system of an avian species. *Journal of Visualized Experiments* 81:e50853.
- Gilch, S., N. Chitoor, Y. Taguchi, M. Stuart, J. E. Jewell, and H. M. Schatzl. 2011. Chronic wasting disease. *Topics in Current Chemistry* 305:51–77.
- Gough, K. C., and B. C. Maddison. 2010. Prion transmission: Prion excretion and occurrence in the environment. *Prion* 4(4):275–282.
- Haley, N. J., S. Carver, L. L. Hoon-Hanks, D. M. Henderson, K. A. Davenport, E. Bunting, S. Gray, B. Trindle, J. Galeota, I. Levan et al. 2014. Detection of chronic wasting disease in the lymph nodes of free-ranging cervids by real-time quaking-induced conversion. *Journal of Clinical Microbiology* 52(9):3237–3243.

- Haley, N. J., R. Donner, D. M. Henderson, J. Tennant, E. A. Hoover, M. Manca, B. Caughey, N. Kondru, S. Manne, A. Kanthasamay et al. 2020. Cross-validation of the RT-QuIC assay for the antemortem detection of chronic wasting disease in elk. *Prion* 14(1): 47–55.
- Haley, N. J., D. M. Henderson, K. Senior, M. Miller, and R. Donner. 2021. Evaluation of winter ticks (*Dermacentor albipictus*) collected from North American elk (*Cervus canadensis*) in an area of chronic wasting disease endemicity for evidence of PrPCWD amplification using real-time quaking-induced conversion assay. *Msphere* 6(4): e00515-21.
- Haley, N. J., C. K. Mathiason, S. Carver, M. Zabel, G. C. Telling, and E. A. Hoover. 2011. Detection of chronic wasting disease prions in salivary, urinary, and intestinal tissues of deer: Potential mechanisms of prion shedding and transmission. *Journal of Virology* 85(13):6309–6318.
- Haley, N. J., D. M. Seelig, M. D. Zabel, G. C. Telling, and E. A. Hoover. 2009. Detection of cwd prions in urine and saliva of deer by transgenic mouse bioassay. *PLoS One*, 4(3):e4848.
- Haley, N. J., C. Siepker, L. L. Hoon-Hanks, G. Mitchell, W. D. Walter, M. Manca, R. J. Monello, J. G. Powers, M. A. Wild, E. A. Hoover et al. 2016a. Seeded amplification of chronic wasting disease prions in nasal brushings and recto-anal mucosa-associated lymphoid tissues from elk by real-time quaking-induced conversion. *Journal of Clinical Microbiology* 54(4):1117–1126.
- Haley, N. J., C. Siepker, W. D. Walter, B. V. Thomsen, J. J. Greenlee, A. D. Lehmkuhl, and J. A. Richt. 2016b. Antemortem detection of chronic wasting disease prions in nasal brush collections and rectal biopsy specimens from white-tailed deer by real-time quaking-induced conversion. *Journal of Clinical Microbiology* 54(4):1108–1116.
- Henderson, D. M., K. A. Davenport, N. J. Haley, N. D. Denkers, C. K. Mathiason, and E. A. Hoover. 2015a. Quantitative assessment of prion infectivity in tissues and body fluids by real-time quaking-induced conversion. *The Journal of general virology* 96(1): 210–219.
- Henderson, D. M., N. D. Denkers, C. E. Hoover, N. Garbino, C. K. Mathiason, and E. A. Hoover. 2015b. Longitudinal detection of prion shedding in saliva and urine by chronic wasting disease-infected deer by real-time quaking-induced conversion. *Journal of Virology* 89(18):9338–9347.

- Henderson, D. M., N. D. Denkers, C. E. Hoover, E. E. McNulty, S. K. Cooper, L. A. Bracchi, C. K. Mathiason, and E. A. Hoover. 2020. Progression of chronic wasting disease in white-tailed deer analyzed by serial biopsy RT-QuIC and immunohistochemistry. *PLoS One* 15(2):e0228327.
- Henderson, D. M., M. Manca, N. J. Haley, N. D. Denkers, A. V. Nalls, C. K. Mathiason, B. Caughey, & E. A. Hoover. (2013). Rapid antemortem detection of CWD prions in deer saliva. *PloS one*, 8(9), e74377.
- Henderson, D. M., J. M. Tennant, N. J. Haley, N. D. Denkers, C. K. Mathiason, and E. A. Hoover. 2017. Detection of chronic wasting disease prion seeding activity in deer and elk feces by real-time quaking-induced conversion. *Journal of General Virology* 98(7):1953–1962.
- Hwang, S., J. J. Greenlee, and E. M. Nicholson. 2021. Real-time quaking-induced conversion detection of prpsc in fecal samples from chronic wasting disease infected white-tailed deer using bank vole substrate. *Frontiers in Veterinary Science* 8:643754.
- John, T. R., H. M. Schatzl, and S. Gilch. 2013. Early detection of chronic wasting disease prions in urine of pre-symptomatic deer by real-time quaking-induced conversion assay. *Prion* 7:253–258.
- Kraft, C. N., N. D. Denkers, C. K. Mathiason, and E. A. Hoover. 2023. Longitudinal detection of prion shedding in nasal secretions of CWD-infected white-tailed deer. *Journal of General Virology* 104(1):001825.
- Kurt, T. D., M. R. Perrott, C. J. Wilusz, J. Wilusz, S. Supattapone, G. C. Telling, M. D. Zabel, and E. A. Hoover. 2007. Efficient in vitro amplification of chronic wasting disease PrP^{res}. *Journal of Virology* 81(17): 9605–9608.
- Lafauci, G., R. I. Carp, H. C. Meeker, X. Ye, J. I. Kim, M. Natelli, M. Cedeno, R. B. Petersen, R. Kascak, and R. Rubenstein. 2006. Passage of chronic wasting disease prion into transgenic mice expressing Rocky Mountain elk (*Cervus elaphus nelsoni*) PrP^c. *Journal of General Virology*, 87(12):3773–3780.

- Li, M. C., M. D. Schwabenlander, G. R. Rowden, J. M. Schefers, C. S. Jennelle, M. Carstensen, D. Seelig, and P. A. Larsen. 2021. RT-QuIC detection of CWD prion seeding activity in white-tailed deer muscle tissues. *Scientific Reports* 11(1):16759.
- Manne, S., N. Kondru, N. Haley, T. Nichols, B. Thomsen, R. Main, P. Halbur, A. Kanthasamy, and A. Kanthasamy. 2015. An independent and blinded confirmation of real-time quaking-induced conversion (RT-QuIC) analysis of cervid rectal biopsies for detection of chronic wasting disease. *Prion* 9:S93–S93.
- Manne, S., N. Kondru, T. Nichols, A. Lehmkuhl, B. Thomsen, R. Main, P. Halbur, S. Dutta, and A. G. Kanthasamy. 2017. Ante-mortem detection of chronic wasting disease in recto-anal mucosa-associated lymphoid tissues from elk (*Cervus elaphus nelsoni*) using real-time quaking-induced conversion (RT-QuIC) assay: A blinded collaborative study. *Prion* 11(6):415–430.
- Mathiason, C. K., J. Hayes-Klug, S. A. Hays, J. Powers, D. A. Osborn, S. J. Dahmes, K. V. Miller, R. J. Warren, G. L. Mason, G. C. Telling et al. 2010. B cells and platelets harbor prion infectivity in the blood of deer infected with chronic wasting disease. *Journal of Virology* 84(10):5097–5107.
- Mathiason, C. K., J. G. Powers, S. J. Dahmes, D. A. Osborn, K. V. Miller, R. J. Warren, G. L. Mason, S. A. Hays, J. Hayes-Klug, D. M. Seelig et al. 2006. Infectious prions in the saliva and blood of deer with chronic wasting disease. *Science* 314(5796):133–136.
- McNulty, E. E., A. V. Nalls, R. Xun, N. D. Denkers, E. A. Hoover, and C. K. Mathiason. 2020. *In Vitro* detection of haematogenous prions in white-tailed deer orally dosed with low concentrations of chronic wasting disease. *Journal of General Virology* 101(3):347–361.
- Miller, M. W., E. S. Williams, N. T. Hobbs, and L. L. Wolfe. 2004. Environmental sources of prion transmission in mule deer. *Emerging infectious diseases* 10(6):1003–1006.
- Moore, S. J., M. H. W. Greenlee, N. Kondru, S. Manne, J. D. Smith, R. A. Kunkle, A. Kanthasamy, and J. J. Greenlee. 2017. Experimental transmission of the chronic wasting disease agent to swine after oral or intracranial inoculation. *Journal of Virology* 91(19):e00926-17.

- Nalls, A. V., E. E. McNulty, A. Mayfield, J. M. Crum, M. K. Keel, E. A. Hoover, M. G. Ruder, and C. K. Mathiason. 2021. Detection of chronic wasting disease prions in fetal tissues of free-ranging white-tailed deer. *Viruses* 13(12):2430.
- Nichols, T. A., J. W. Fischer, T. R. Spraker, Q. Kong, and K. C. Vercauteren. 2015. CWD prions remain infectious after passage through the digestive system of coyotes (*Canis latrans*). *Prion* 9(5):367–375.
- Nichols, T. A., B. Pulford, A. C. Wyckoff, C. Meyerett, B. Michel, K. Gertig, E. A. Hoover, J. E. Jewell, G. C. Telling, and M. D. Zabel. 2009. Detection of protease-resistant cervid prion protein in water from a CWD-endemic area. *Prion* 3(3):171–183.
- Oravcova, V., A. Ghosh, L. Zurek, J. Bardon, S. Guenther, A. Cizek, and I. Literak. 2013. Vancomycin-resistant enterococci in rooks (*Corvus frugilegus*) wintering throughout Europe. *Environmental microbiology* 15(2):548–556.
- Oravcova, V., L. Zurek, A. Townsend, A. B. Clark, J. C. Ellis, A. Cizek, and I. Literak. 2014. American crows as carriers of vancomycin-resistant enterococci with vanA gene. *Environmental microbiology* 16(4):939–949.
- Pennsylvania Game Commission. 2020. Pennsylvania chronic wasting disease response plan. <<https://www.pgc.pa.gov/Wildlife/WildlifeHealth/Documents/Final%20CWD%20Response%20Plan%20July%202020.pdf>>. Accessed 30 Oct 2024.
- Plummer, I. H., C. J. Johnson, A. R. Chesney, J. A. Pedersen, and M. D. Samuel. 2018. Mineral licks as environmental reservoirs of chronic wasting disease prions. *PLoS One* 13(5):e0196745.
- Prior, K. A., and P. J. Weatherhead. 1991. Competition at the carcass: Opportunities for social foraging by turkey vultures in southern Ontario. *Canadian Journal of Zoology* 69(6):1550–1556.
- Prusiner, S. B. 1998. Prions. *Proceedings of the National Academy of Sciences of the United States of America*, 95(23):13363–13383.
- Pulford, B., T. R. Spraker, A. C. Wyckoff, C. Meyerett, H. Bender, A. Ferguson, B. Wyatt, K. Lockwood, J. Powers, G. C. Telling et al. 2012. Detection of prpCWD in feces from naturally exposed Rocky

- Mountain elk (*Cervus elaphus nelsoni*) using protein misfolding cyclic amplification. *Journal of Wildlife Diseases* 48(2):425–434.
- Safar, J. G., P. Lessard, G. Tamguney, Y. Freyman, C. Deering, F. Letessier, S. J. Dearmond, and S. B. Prusiner. 2008. Transmission and detection of prions in feces. *Journal of Infectious Diseases* 198(1):81–89.
- Sohn, H. J., J. H. Kim, K. S. Choi, J. J. Nah, Y. S. Joo, Y. H. Jean, S. W. Ahn, O. K. Kim, D. Y. Kim, and A. Balachandran. 2002. A case of chronic wasting disease in an elk imported to Korea from Canada. *Journal of Veterinary Medical Science* 64(9):855–858.
- Tamguney, G., M. W. Miller, L. L. Wolfe, T. M. Sirochman, D. V. Glidden, C. Palmer, A. Lemus, S. J. Dearmond, and S. B. Prusiner. 2009. Asymptomatic deer excrete infectious prions in faeces. *Nature* 461(7263):529–532.
- Tamguney, G., J. A. Richt, A. N. Hamir, J. J. Greenlee, M. W. Miller, L. L. Wolfe, T. M. Sirochman, A. J. Young, D. V. Glidden, N. L. Johnson et al. 2012. Salivary prions in sheep and deer. *Prion* 6(1): 52–61.
- Tamguney, G. L., K. Giles, E. Bouzamondo-Bernstein, P. J. Bosque, M. W. Miller, J. Safar, S. J. Dearmond, and S. B. Prusiner. 2006. Transmission of elk and deer prions to transgenic mice. *Journal of Virology* 80(18):9104–9114.
- Tewari, D., M. Fasnacht, M. Ritzman, J. Livengood, J. Bower, A. Lehmkuhl, T. Nichols, A. Hamberg, K. Brightbill, and D. Henderson. 2022. Detection of chronic wasting disease in feces and recto-anal mucosal associated lymphoid tissues with RT-QuIC in a naturally infected farmed white-tailed deer herd. *Frontiers in Veterinary Science* 9:959555.
- Tewari, D., D. Steward, M. Fasnacht, and J. Livengood. 2021. Detection by real-time quaking-induced conversion (RT-QuIC), ELISA, and IHC of chronic wasting disease prion in lymph nodes from Pennsylvania white-tailed deer with specific PRNP genotypes. *Journal of Veterinary Diagnostic Investigation* 33(5):943–948.

- Trifilo, M. J., G. Ying, C. Teng, and M. B. A. Oldstone. 2007. Chronic wasting disease of deer and elk in transgenic mice: Oral transmission and pathobiology. *Virology* 365(1):136–143.
- USDA.2024. National Veterinary Accreditation Program Reference Guide: Issuing USDA APHIS. United States of America.
- Vercauteren, K. C., J. L. Pilon, P. B. Nash, G. E. Phillips, and J. W. Fischer. 2012. Prion remains infectious after passage through digestive system of american crows (*Corvus brachyrhynchos*). *PLoS One* 7(10):e45774.
- Williams, E. S., and S. Young. 1980. Chronic wasting disease of captive mule deer: A spongiform encephalopathy. *Journal of Wildlife Diseases* 16(1):89–98.

Table 1.1 Summary of real time quaking induced conversion analysis that resulted in positive chronic wasting disease detections categorized by sample material and species sampled.

Sample material	Species	Reference
Lymph nodes	White-tailed deer (<i>Odocoileus virginianus</i>), Mule deer (<i>Odocoileus hemionus</i>), Moose(<i>Alces alces</i>)	Haley et al. 2014; Tewari et al. 2021
Saliva	White-tailed deer	Henderson et al. 2015b; Henderson et al. 2013
Blood	White-tailed deer, Muntjak (<i>Muntiacus muntjak</i>), Hamster (<i>Mesocricetus auratus</i>)	Elder et al., 2013,2015; McNulty et al. 2020
Urine	White-tailed deer, Mule deer	Henderson et al. 2015b; John et al. 2013
Feces	White-tailed deer, Elk (<i>Cervus canadensis</i>)	Cheng et al. 2016, 2017; Henderson et al. 2017; Hwang et al. 2021
Rectoanal mucosa-associated lymphoid tissue	White-tailed deer, Elk	Haley et al. 2016a, 2016b; Henderson et al. 2020; Manne et al. 2015, 2017; Tewari et al. 2022
Nasal brushings	White-tailed deer, Elk	Haley et al. 2016a, 2016b; Kraft et al. 2023
Third eyelid	White-tailed deer, Elk	Cooper et al. 2019
Ear tissue	White-tailed deer, Mule deer	Ferreira et al. 2021
Tonsils	White-tailed deer	Henderson et al. 2020
Fetal tissue	White-tailed deer	Nalls et al. 2021
Tongue	White-tailed deer	Li et al. 2021
Neck muscle	White-tailed deer	Li et al. 2021
Engorged tick	Elk	Haley et al. 2021

Table 1.2 Summary of bioassay performed with chronic wasting disease prions from an infected species (Species) that resulted in disease transmission identifying sample material of inoculum (Sample material), species inoculated (Bioassay), inoculation method, and source (Reference).

Species	Sample material	Bioassay	Inoculation method	Reference
White-tailed deer (<i>Odocoileus virginianus</i>)	Brain	Transgenic mice	Intracranial Injection	Tamguney et al. 2006
		Swine (<i>Sus domesticus</i>)	Intracranial injection, Oral inoculation	Moore et al. 2017
	Blood	White-tailed deer	Intracranial injection, Intravenous injection, Intraperitoneal injection, Oral inoculation	Mathiason et al. 2010
	Saliva	Transgenic mice	Intracranial Injection	Haley et al. 2009
	Urine	Transgenic mice	Intracranial Injection	Haley et al. 2009
Mule deer (<i>Odocoileus hemionus</i>)	Brain	Transgenic mice	Intracranial injection, Oral inoculation, Aerosolized inoculation, Inter-nasal inoculation	Browning et al. 2004; Denkers et al. 2010; Lafauci et al. 2006; Tamguney et al. 2006; Trifilo et al. 2007
		White-tailed deer	Intravenous injection, Intraperitoneal	Mathiason et al. 2006
	Blood	White-tailed deer	Intravenous injection, Intraperitoneal	Mathiason et al. 2006
	Saliva	White-tailed deer	Intravenous injection, Intraperitoneal	Mathiason et al. 2006
	Feces	Transgenic mice	Intracranial injection	Tamguney et al. 2009
Elk (<i>Cervus canadensis</i>)	Brain	Transgenic mice	Intracranial injection	Angers et al. 2009; Browning et al. 2004; Lafauci et al. 2006; Tamguney et al.,2006
	Velvet	Transgenic mice	Intracranial injection	Angers et al. 2009
Coyote (<i>Canis latrans</i>)	Feces	Transgenic mice	Intracranial injection	Nichols et al. 2015
Transgenic mice	Brain	Transgenic mice	Intracranial injection	Lafauci et al. 2006

Table 1.3 Real time quaking induced conversion assay results from American crow (*Corvus brachyrhynchos*) fecal and cloacal samples collected with a 10⁻³ dilution, including multiple thresholds of detection in Pennsylvania, USA, 2023-2024.

Individual ID	Swab type	5X Standard deviation threshold				10X Standard deviation threshold			
		Run 1	Run 2	Run 3	Total	Run 1	Run 2	Run 3	Total
AMCR001	Fecal	4/6	6/6	1/6	11/18	0/6	0/6	0/6	0/18
	Cloacal	0/6	6/6	0/6	6/18	0/6	1/6	0/6	1/18
AMCR002	Fecal	3/6	2/6	0/6	5/18	0/6	0/6	0/6	0/18
AMCR003	Fecal	0/6	0/6	0/6	0/18	0/6	0/6	0/6	0/18
	Cloacal	0/6	0/6	0/6	0/18	0/6	0/6	0/6	0/18
AMCR004	Fecal	0/6	1/6	0/6	1/18	0/6	1/6	0/6	1/18
	Cloacal	2/6	0/6	1/6	3/18	0/6	0/6	1/6	1/18
AMCR005	Fecal	6/6	6/6	6/6	18/18	1/6	6/6	1/6	8/18
	Cloacal	3/6	0/6	0/6	3/18	0/6	0/6	0/6	0/18
AMCR006	Cloacal	0/6	0/6	0/6	0/18	0/6	0/6	0/6	0/18
AMCR007	Fecal	6/6	0/6	0/6	6/18	2/6	0/6	0/6	2/18
	Cloacal	0/6	0/6	0/6	0/18	0/6	0/6	0/6	0/18
AMCR008	Cloacal	0/6	0/6	0/6	0/18	0/6	0/6	0/6	0/18
AMCR009	Fecal	0/6	0/6	0/6	0/18	0/6	0/6	0/6	0/18
	Cloacal	6/6	5/6	1/6	12/18	0/6	0/6	1/6	1/18
AMCR010	Fecal	0/6	0/6	0/6	0/18	0/6	0/6	0/6	0/18
	Cloacal	0/6	3/6	0/6	3/18	0/6	0/6	0/6	0/18
AMCR011	Fecal	3/6	1/6	5/6	9/18	0/6	0/6	0/6	0/18
	Cloacal	0/6	4/6	0/6	4/18	0/6	0/6	0/6	0/18
AMCR012	Fecal	6/6	1/6	0/6	7/18	6/6	1/6	0/6	7/18
	Cloacal	0/6	1/6	0/6	1/18	0/6	1/6	0/6	1/18
AMCR013	Cloacal	0/6	0/6	4/6	4/18	0/6	0/6	4/6	4/18
AMCR014	Fecal 1	6/6	6/6	6/6	18/18	2/6	0/6	0/6	2/18
	Fecal 2	6/6	6/6	6/6	18/18	6/6	0/6	0/6	6/18
	Cloacal	1/6	0/6	0/6	1/18	1/6	0/6	0/6	1/18
AMCR015	Cloacal	0/6	0/6	0/6	0/18	0/6	0/6	0/6	0/18

Table 1.4 Real time quaking induced conversion assay results from fish crow (*Corvus ossifragus*) fecal and cloacal samples with a 10⁻³ dilution, including multiple thresholds of detection in Pennsylvania, USA, 2023-2024.

Individual ID	Swab type	5X Standard deviation threshold				10X Standard deviation threshold			
		Run 1	Run 2	Run 3	Total	Run 1	Run 2	Run 3	Total
FICR001	Cloacal	1/6	5/6	0/6	6/18	0/6	0/6	0/6	0/18
FICR002	Cloacal	0/6	0/6	0/6	0/18	0/6	0/6	0/6	0/18
FICR003	Cloacal	0/6	0/6	0/6	0/18	0/6	0/6	0/6	0/18
FICR004	Cloacal	6/6	6/6	6/6	18/18	0/6	6/6	4/6	10/18
FICR005	Cloacal	3/6	6/6	0/6	9/18	0/6	6/6	0/6	6/18
FICR006	Cloacal	2/6	6/6	1/6	9/18	0/6	6/6	1/6	7/18
FICR007	Cloacal	3/6	6/6	1/6	10/18	0/6	6/6	0/6	6/18
FICR008	Cloacal	0/6	0/6	0/6	0/18	0/6	0/6	0/6	0/18
FICR009	Fecal	6/6	6/6	5/6	17/18	0/6	6/6	0/6	6/18
	Cloacal	0/6	0/6	0/6	0/18	0/6	0/6	0/6	0/18
FICR010	Cloacal	0/6	1/6	0/6	1/18	0/6	1/6	0/6	1/18
FICR011	Cloacal	6/6	6/6	5/6	17/18	0/6	6/6	1/6	7/18
FICR012	Cloacal	1/6	6/6	0/6	7/18	1/6	0/6	0/6	1/18
FICR013	Cloacal	1/6	6/6	0/6	7/18	0/6	1/6	0/6	1/18
FICR014	Cloacal	6/6	6/6	6/6	18/18	6/6	6/6	6/6	18/18
FICR015	Cloacal	5/6	0/6	2/6	7/18	0/6	6/6	0/6	6/18
FICR016	Cloacal	2/6	0/6	0/6	2/18	0/6	0/6	0/6	0/18
FICR017	Cloacal	2/6	0/6	0/6	2/18	0/6	0/6	0/6	0/18
FICR018	Cloacal	2/6	0/6	2/6	4/18	0/6	0/6	2/6	2/18
FICR019	Cloacal	0/6	0/6	1/6	1/18	0/6	0/6	1/6	1/18
FICR020	Fecal	0/6	2/6	3/6	5/18	0/6	2/6	3/6	5/18
	Cloacal	1/6	1/6	2/6	4/18	1/6	1/6	2/6	4/18
FICR021	Fecal	6/6	6/6	6/6	18/18	6/6	2/6	5/6	13/18
	Cloacal	0/6	0/6	0/6	0/18	0/6	0/6	0/6	0/18
FICR022	Cloacal	0/6	0/6	0/6	0/18	0/6	0/6	0/6	0/18
FICR023	Cloacal	0/6	0/6	0/6	0/18	0/6	0/6	0/6	0/18

Table 1.5 Real time quaking induced conversion assay results from opportunistic fecal samples with a 10⁻³ dilution, including multiple runs and multiple thresholds of detection in Pennsylvania, USA, 2023-2024.

Sample ID	5X Standard deviation threshold				10X Standard deviation threshold			
	Run 1	Run 2	Run 3	Total	Run 1	Run 2	Run 3	Total
FS001	0/6	0/6	0/6	0/18	0/6	0/6	0/6	0/18
FS002	6/6	6/6	6/6	18/18	2/6	0/6	0/6	2/18
FS003	1/6	0/6	0/6	1/18	1/6	0/6	0/6	1/18
FS004	6/6	6/6	6/6	18/18	1/6	2/6	1/6	4/18
FS005	1/6	0/6	1/6	2/18	1/6	0/6	1/6	2/18
FS006	0/6	0/6	1/6	1/18	0/6	0/6	1/6	1/18
FS007	0/6	0/6	0/6	0/18	0/6	0/6	0/6	0/18
FS008	6/6	6/6	6/6	18/18	6/6	6/6	6/6	18/18
FS009	0/6	1/6	6/6	1/18	0/6	1/6	0/6	1/18

Table 1.6 Real time quaking induced conversion assay results with total number of wells and proportion of wells that crossed the threshold for American crows (AMCR; *Corvus brachyrhynchos*) and fish crows (FICR; *Corvus ossifragus*) as well as positive and negative controls in Pennsylvania, USA, 2023-2024.

Sample type	Sample material	Total sample wells	Wells that cross the 5X threshold		Wells that cross the 10X threshold	
AMCR	Fecal	216	93	43.0556%	26	12.0370%
	Cloacal	252	37	14.6825%	9	3.5714%
	All	468	130	27.7778%	35	7.4786%
FICR	Fecal	54	40	74.0741%	24	44.4444%
	Cloacal	414	122	29.4686%	70	16.9082%
	All	468	162	34.6154%	94	20.0855%
Opportunistic	Fecal	162	59	36.4198%	29	17.9012%
All samples	Fecal	432	192	44.4444%	79	18.2870%
	Cloacal	666	159	23.8739%	79	11.8619%
	All	1098	351	31.9672%	158	14.3898%
Lymph nodes	Positive	42	42	100.0000%	42	100.0000%
	Negative	41	7	17.0732%	3	7.3171%

Figure 1.1 Real-time quaking-induced conversion assay results from American crow (*Corvus brachyrhynchos*) fecal samples in Pennsylvania, USA, 2023-2024. For each individual 18 replicate wells were tested and the number of wells that exceeded the fluorescence threshold is represented in blue and the wells that did not exceed the threshold are represented in gray. A) 5X threshold; B) 10X threshold.

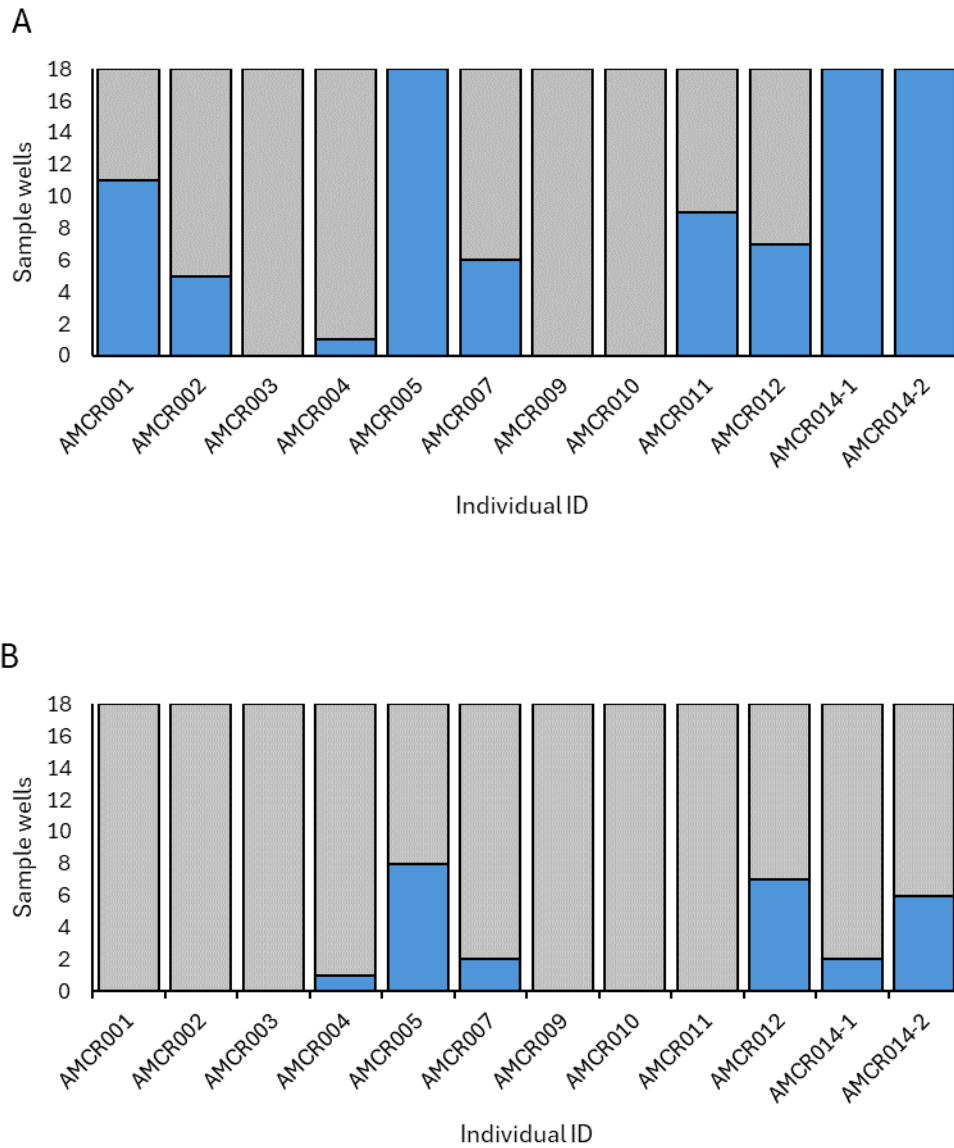


Figure 1.2 Real-time quaking-induced conversion assay results from American crow (*Corvus brachyrhynchos*) cloacal samples in Pennsylvania, USA, 2023-2024. For each individual 18 replicate wells were tested and the number of wells that exceeded the fluorescence threshold is represented in green and the wells that did not exceed the threshold are represented in gray. A) 5X threshold; B) 10X threshold.

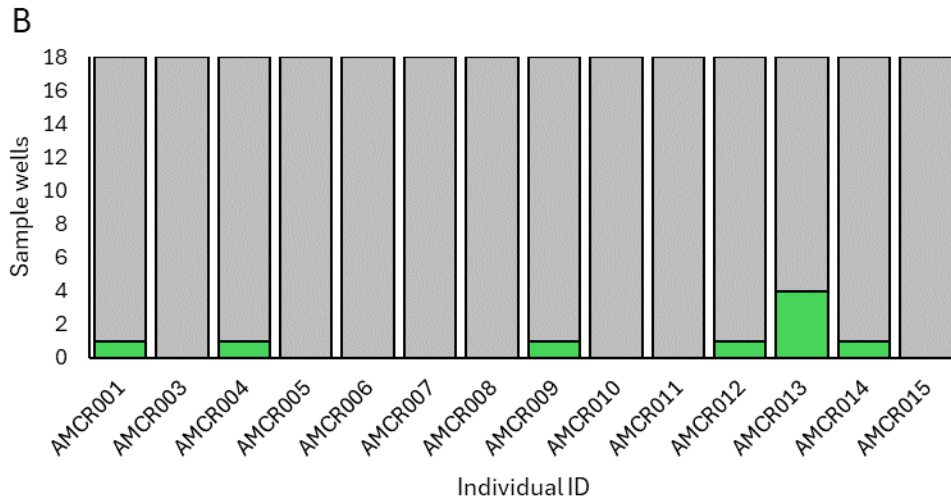
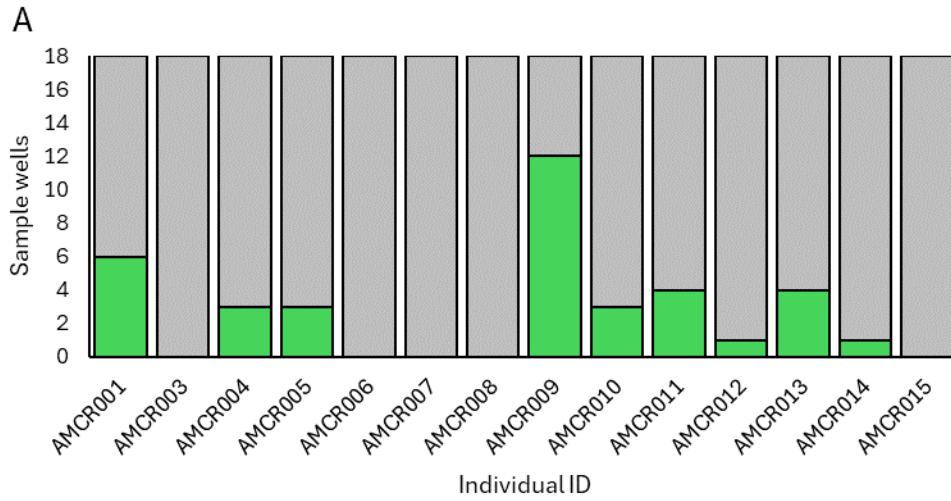


Figure 1.3 Real-time quaking-induced conversion assay results from fish crow (*Corvus ossifragus*) fecal and cloacal samples in Pennsylvania, USA, 2023-2024. For each sample 18 replicate wells were tested and the number of wells that exceeded the fluorescence threshold is represented in purple for fecal samples and dark blue for cloacal samples, the wells that did not exceed the threshold are represented in gray. A) 5X threshold; B) 10X threshold.

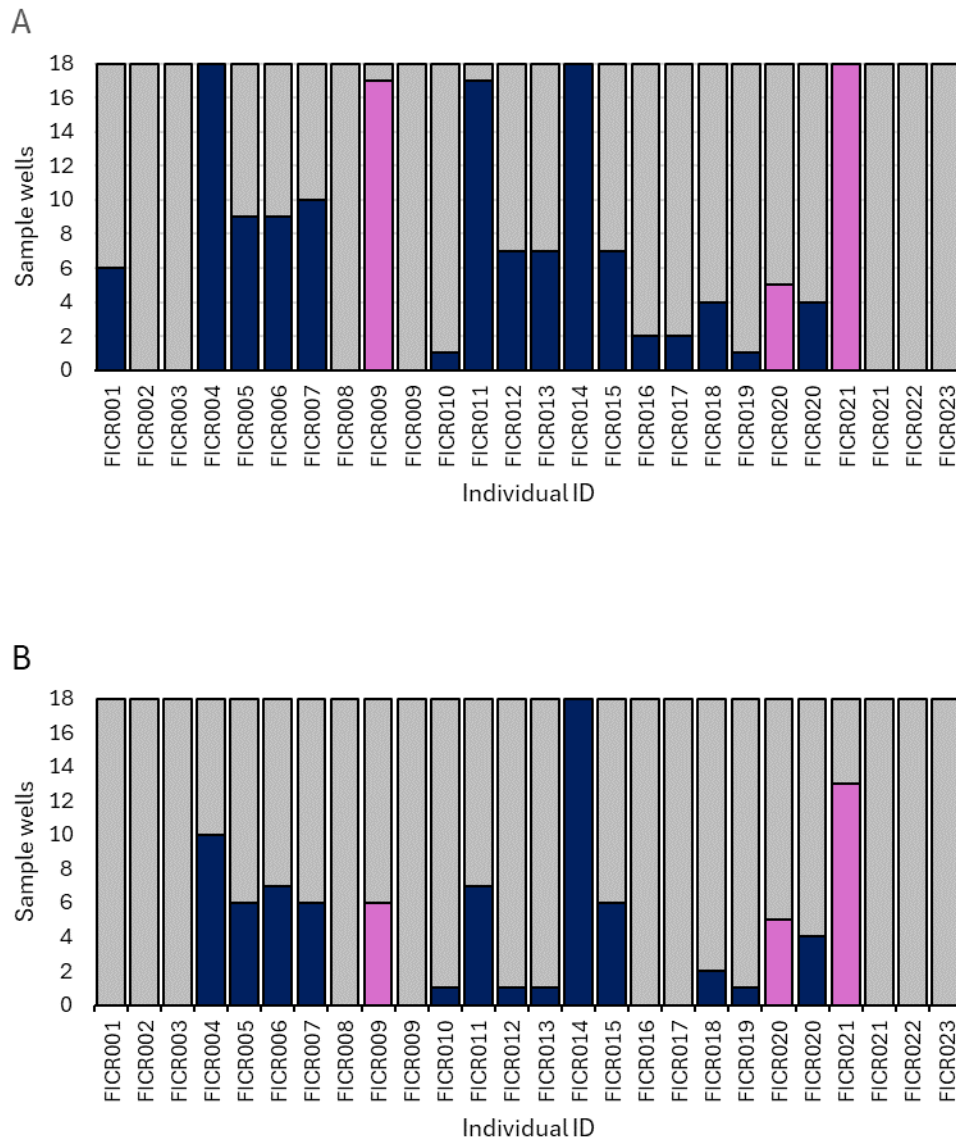


Figure 1.4 Fluorescence of real-time quaking-induced conversion assay for samples of American crow (*Corvus brachyrhynchos*) feces (blue) in Pennsylvania, USA, 2023-2024, with positive controls (red), and negative controls (yellow). Threshold values are included for the 5X threshold (gray), and 10X threshold (black) A) The fluorescence values including the maximum values for these sample wells; B) A focused view of the sample well fluorescence in relation to the threshold values.

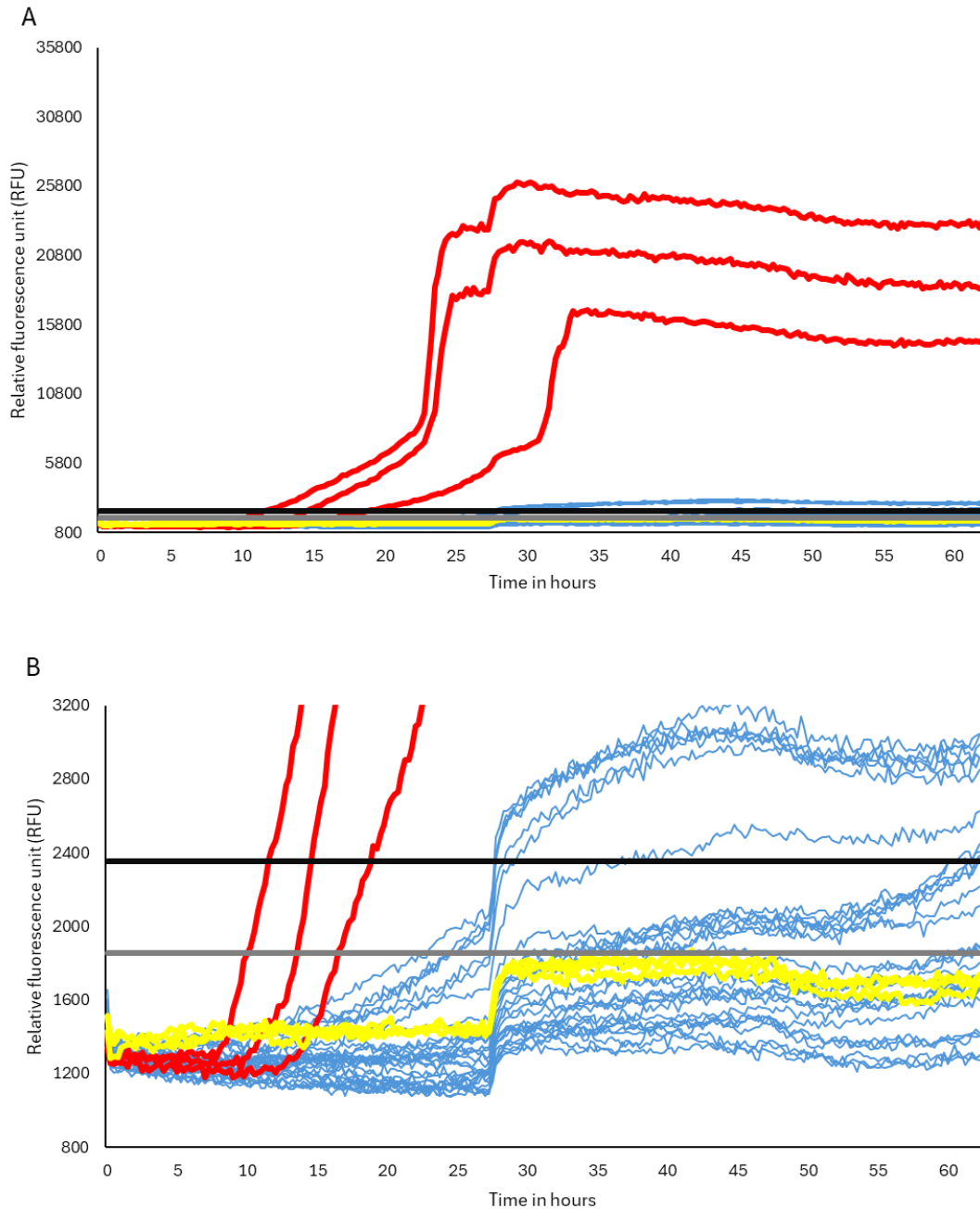


Figure 1.5 Fluorescence of real-time quaking-induced conversion assay for samples of American crow (*Corvus brachyrhynchos*) cloacal swabs (green) in Pennsylvania, USA, 2023-2024, with positive controls (red), and negative controls (yellow). Threshold values are included for the 5X threshold (gray), and 10X threshold (black) A) The fluorescence values including the maximum values for these sample wells. B) A focused view of the sample well fluorescence in relation to the threshold values.

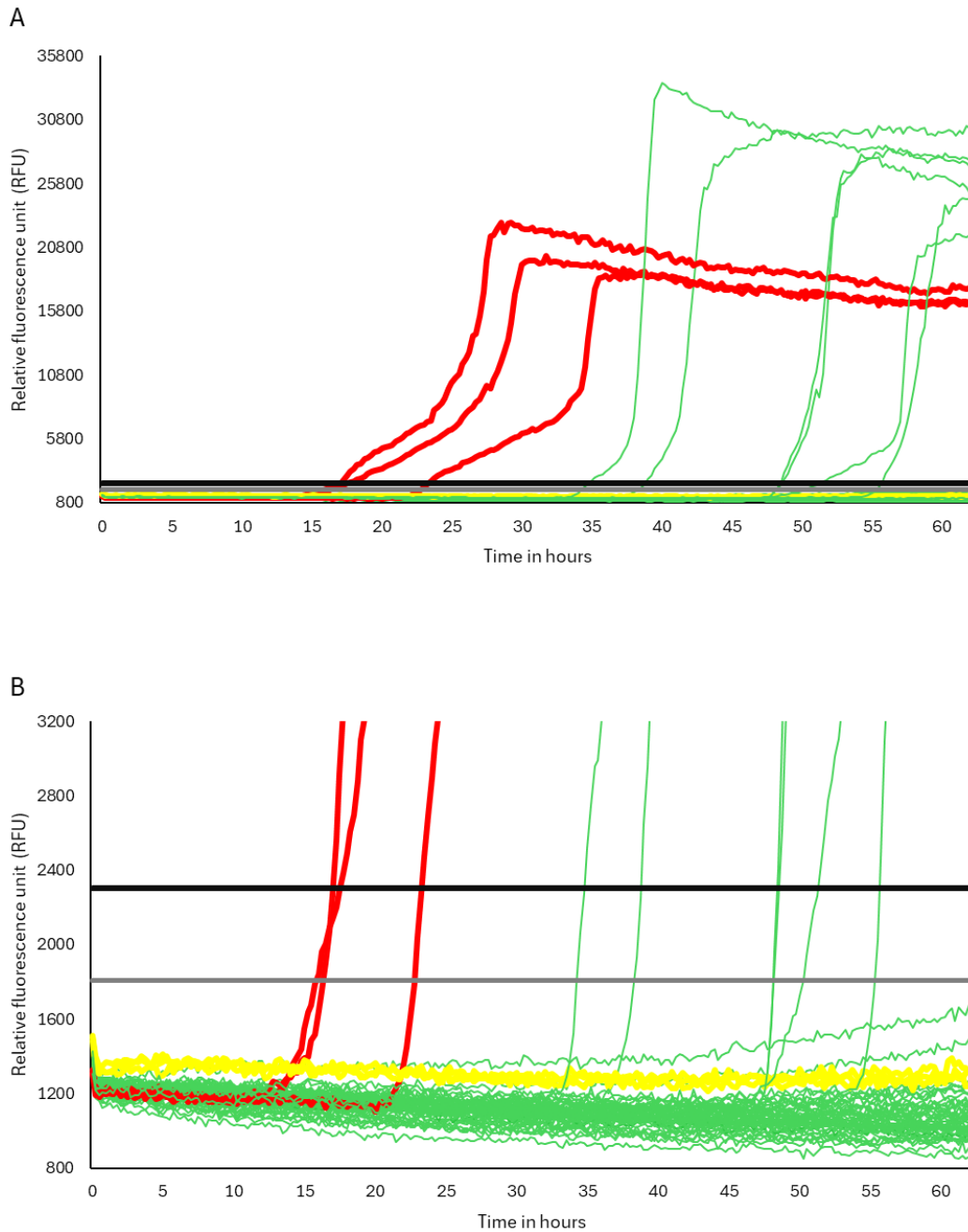
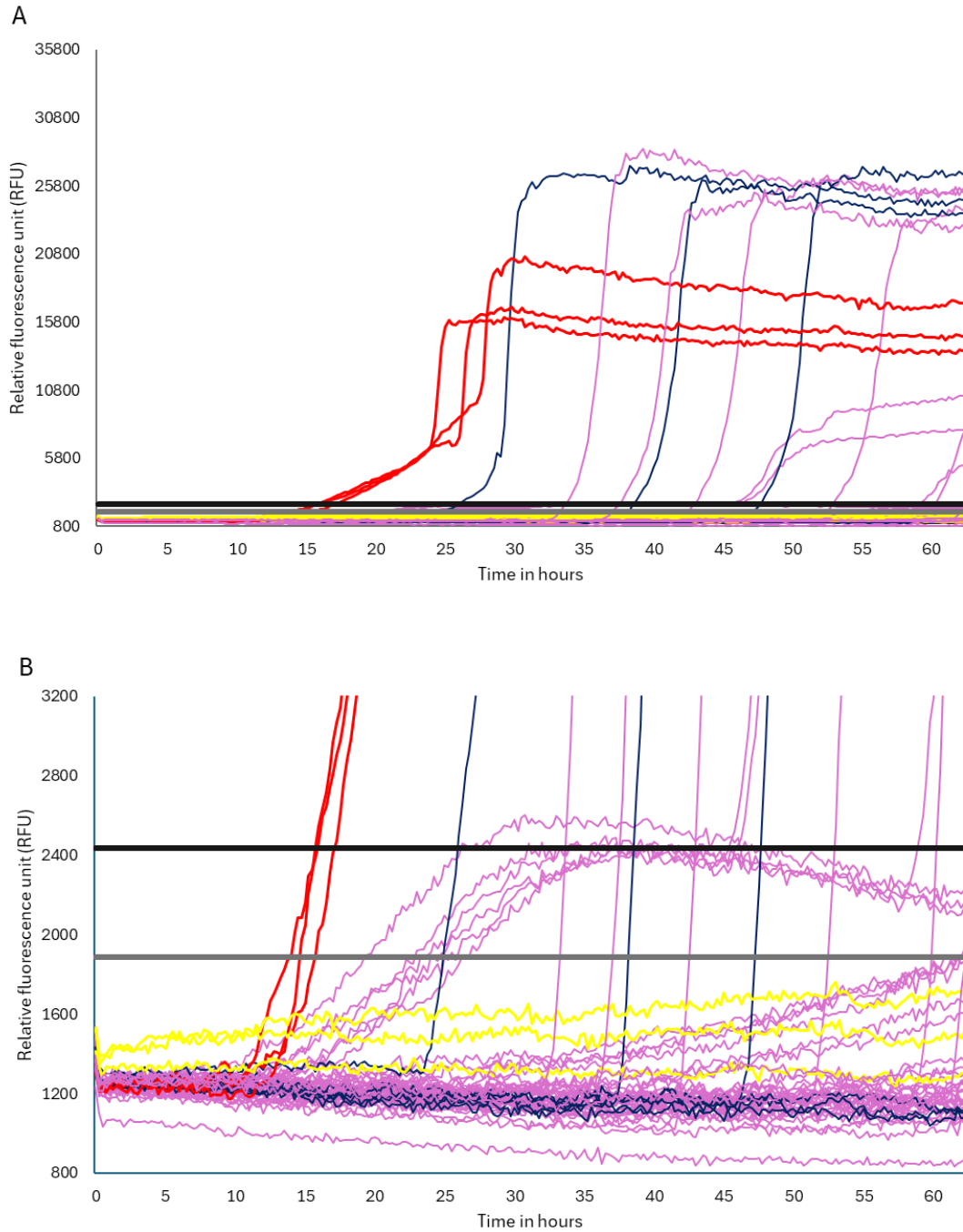


Figure 1.6 Fluorescence of real-time quaking-induced conversion assay for samples of fish crow (*Corvus ossifragus*) feces (purple) and cloacal swabs (dark blue) in Pennsylvania, USA, 2023-2024, with positive controls (red), and negative controls (yellow). Threshold values are included for the 5X threshold (gray), and 10X threshold (black) A) The fluorescence values including the maximum values for these sample wells. B) A focused view of the sample well fluorescence in relation to the threshold values.



Chapter 2

Resource use by American crow (*Corvus brachyrhynchos*) surrounding an area endemic for chronic wasting disease.

Chapter 2 was written in collaboration with Kurt C. VerCauteren and W. David Walter. I have included this manuscript on the following pages as formatted for the Journal of Wildlife Management.

ABSTRACT

American crows (*Corvus brachyrhynchos*) are a common species found throughout North America. Crows play a role in the ecology of multiple diseases and laboratory experiments have shown the potential for crows to pass infectious prions, such as those associated with chronic wasting disease (CWD), in their feces after being gavaged with infected meat. This has not yet been documented in a wild setting; however, research on crow space use and resource selection may provide a better understanding of their potential role in the movement of infectious prions. We captured 15 American crows and outfitted them with global positioning system (GPS) transmitters to record locations at 10-minute intervals. We used GPS data to calculate estimates of home range size using Brownian bridge movement models, dynamic Brownian bridge movement models, movement-based kernel density, and kernel density with iterative plug-in bandwidth selection. In addition, we performed integrated step selection function with covariates representing habitat type, potential sources of prion-infected material (e.g., dump bin for harvested deer), and landscape features. We found a high level of variability between individual crows 95% home range estimates, which ranged from 0.76 km² to 346.7 km². There was also a diversity of covariates included in the model of best fit for individual crows suggesting that crows differed individually in their space use and resource use. We documented individual crows interacting with locations where CWD prions may be present including captive cervid facilities and carcass disposal bins as well as some individuals crossing back and forth across CWD disease management area boundaries highlighting their potential role in disease movement.

KEYWORDS American crows, Brownian bridge, chronic wasting disease, *Corvus brachyrhynchos*, home range estimation, integrated step selection function, Pennsylvania

INTRODUCTION

Avian species play many roles within their ecosystem, including the movement of various materials. Seed eating birds act as agents of dispersal for a variety of plants, movements of these birds shape the structure and composition of their environment (Nathan and Muller-Landau 2000), and bird seed dispersal can even contribute to the colonization of isolated island environments (Proctor 1968). Predatory birds that consume seed eating birds also contribute to seed dispersal (Padilla et al. 2012). Avian species are biological disease vectors as well as mechanical vectors through transport of disease agents on their feathers and feet for diseases that impact plants, other wildlife, livestock, and humans including but not limited to; highly pathogenic avian influenza H5N1 virus (Gaidet et al. 2010), *Escherichia coli* (Sen et al. 2020), chytrid fungus (*Batrachochytrium dendrobatidis*; Hanlon et al. 2017; Garmyn et al. 2012), *Campylobacter jejuni* (Taff et al. 2016), tick borne pathogens (de la Fuente et al. 2015), West Nile virus (*Orthoflavivirus nilense*; Wilcox et al. 2007; Yaremych et al. 2004a), *Phytophthora* (Malewski et al. 2019), *Avipoxvirus* (Wilcox et al. 2007; Yaremych et al. 2004a), and *Collyriclum faba* (Grove et al. 2005). Understanding the space use of birds is essential to understanding the ecology of ecosystems they inhabit. Global positioning system (GPS) transmitter technology can provide frequent observations of locations which enables in depth analysis of bird space use and interactions with the landscape. The ability to collect this data has been limited by the size and weight of available transmitters; however, smaller transmitters have been developed and are becoming more readily available, which has expanded the number of species that can be tracked with GPS transmitters.

American crows (*Corvus brachyrhynchos*) are capable of carrying modern GPS transmitters and are of great interest as they are known carriers of numerous diseases. In addition, a laboratory study demonstrated that crows gavaged with meat containing infectious prions responsible for scrapie can subsequently shed the prions in their feces (Vercauteren et al. 2012). These findings have not been replicated through samples acquired from wild birds on the landscape so studying crow space use and resource selection in areas endemic for prion disease is important in assessing their potential role in the

movement of infectious prions. Chronic wasting disease (CWD) is a fatal prion disease in cervids that was first detected in Colorado in 1967 (Williams and Young 1980) and has been documented since 2012 in Pennsylvania in both wild and captive white-tailed deer (*Odocoileus virginianus*) which is a species of economic and cultural importance (Pennsylvania Game Commission 2020)

Spatial ecology of American crows has been studied extensively throughout North America with the use of very high frequency (VHF) telemetry. Size of home range estimates using VHF have varied across study sites and estimator of home range used. In Manitoba, Canada a sample of 10 crows had an average home range size of 2.6 km² using minimum convex polygons (MCP; Sullivan and Dinsmore 1992). A sample of 45 crows, with an average of 48 locations per individual, in Illinois, United States had a mean 95% home range size of 7.6 km² using MCP (Yaremych et al. 2004b). Fixed kernel estimation with least squares cross validation has also been used with VHF location data yielding an average home range size estimate of 3.21 km² for a sample of 39 crows in Washington, United States (Neatherlin et al. 2004). Resource selection analysis of crows from a combination of visual observations and 13 individuals with VHF transmitters in Washington, United States identified many factors influencing their landscape use, including level of urbanization, land use, and availability of major food resources, such as agricultural fields or landfills (Withey and Marzluff 2008). Crows have also been shown to preferentially roost in urban areas while selecting for agricultural land cover for foraging grounds (Yaremych et al. 2004b).

There has so far been limited use of GPS transmitters on American crows in estimation of size of home range or resource use. Townsend et al. (2018) used satellite tags on 18 crows collecting a total of 11,951 locations across 1,305 days to assess questions regarding crow migration. In Davis, California Taff et al. (2016) monitored 8 crows with GPS transmitters recording 9 locations a day for 3 months yielding a total of 2,147 locations and estimated home ranges using MCP for 7 individuals identifying a mean size of 235 km² (range: 78-684 km²). Crows selected for fallow fields, grasslands, hay fields, almond trees, walnut trees, and areas of medium or high intensity development and avoided tomatoes,

winter wheat, sunflower, alfalfa, rice, and other crops (Taff et al. 2016). Additionally, crows showed a significant preference for a primate research center and dairy cattle barn. Our objective is to study crow space use in an area endemic for CWD. We expect home range size to differ between individuals in our study as previous studies have shown variability between individual crows. We predict resource selection will identify important resources for crows within our study area including those where CWD prions may be present.

STUDY AREA

Our study area was in Blair, Bedford, Cambria, Franklin, Fulton, Huntingdon, and Somerset counties in central Pennsylvania, United States. We concentrated our study area within Disease Management Area 2 (DMA 2) that was established by the Pennsylvania Game Commission (PGC) was in response to detection of CWD in wild and captive deer in 2012 that has expanded in subsequent years due to additional detections of positive deer (Pennsylvania Game Commission 2020)

METHODS

Capture

We captured crows with a variety of trap types and a variety of foods as bait to attract and entice crows to remain at a trap. A netlauncher (Coda Enterprises, Inc., Mesa, AZ) is a common tool used in avian capture for both research and nuisance purposes (Prisock et al. 2012) that uses a blank round to project a net over birds feeding at a bait pile strategically placed for capture effectiveness and animal safety. We activated the netlauncher remotely, while on-site, via an electronic trigger. This capture sequence gave us control over when the netlauncher was detonated to eliminate risk of trapping non-target species and ensuring capture occurred as safely as possible.

We modified clover traps (Wildlife Capture Services, LLC, Flagstaff, Arizona), typically used to capture white-tailed deer, to function as walk in style traps for capturing crows. We altered the trap geometry to increase the interior height and enabled dual functionality so two traps could be used

independently but also easily joined as one larger trap. In addition, we outfitted the traps with a remote door closure system that could be remotely triggered from several hundred feet. Walk-in traps with a remote trigger have been used previously to trap crows (Caffrey 2002) and our custom design was successful after extensive trial and error observing the behavior of crows in response to these traps. Bownets (Mike's Falconry Supplies, Sandy, Oregon) with a remote trigger were also used as a physical restraint capture method, although this was mostly ineffective as a capture method. The remote trigger system allowed the trap to be triggered from a distance of over 100 meters without disturbing the crows; however, on some occasions the crows were able to flee faster than the net closure mechanism could close the net.

Australian ladder traps are semi-permanent structures that allow for the capture of multiple crows at a time (Kalmbach and Aldous 1940) and can be monitored remotely. After observing crows interact with different opening sizes of the Australian ladder trap, we spaced the ladder rungs 14.1 cm apart for capture as American crows easily dropped in and then had difficulty exiting the trap with this spacing. We used food-based attractants and monitored the traps with cellular motion activated trail cameras (PRADCO Outdoor Brands, Birmingham, Alabama).

Transmitters and banding

We equipped captured crows with backpack harnesses that included OrniTrack-10 solar powered GPS transmitters (Ornitela, Vilnius, Lithuania) that weighed 10 grams and have built in solar panels to extend the life of the transmitter. The transmitters recorded GPS locations and accelerometry data at 10-minute intervals from nautical dawn to nautical dusk which was uploaded via the global system for mobile communications network. Longer intervals between recorded locations did occur during periods of reduced solar charging. We collected data for each individual until detachment of the transmitter or death of the bird. We constructed the harnesses using 1 mm rattail cord to create two loops from the back of the bird around the sternum, one below the wings and one around the neck. We connected the loops along the keel of the bird with a rubber tube-encased thread breakaway link. These breakaway links reduce risk of

bird entanglement or harness related injury and mortality (Karl and Clout 1987). We selected transmitters without external antennae to prevent crows from being able to remove or tamper with the transmitter. We adhered to the guidelines of the USGS Bird Banding Laboratory (BBL) that transmitter and harness materials total weight was <3% of body weight of an individual and did not place a transmitter on a bird that weighed under 415 grams.

We marked captured crows using metal leg bands of either size 5 or 4A depending on the size of the individuals' legs as recommended by BBL. When multiple individuals were captured at a single site and weight restrictions allowed (birds weighing over 470 grams), we also marked individuals with BBL approved color bands to allow for identification via direct observation. Our GPS transmitters do not have VHF capabilities to track individuals, so color banding enabled the identification of tagged individuals observed foraging or in communal roosts.

In the event that GPS data, location, and accelerometer of a crow showed a prolonged lack of movement indicating a possible mortality event or a transmitter drop off, we made an effort to gain access to that location to recover the transmitter. We labeled all transmitters with an email address for individuals to contact us if found. Our work was approved by the Pennsylvania State University Institutional Animal Care and Use Committee permit PROTO202102055. All bird capture and banding were done in accordance with BBL guidelines and authorized through permit 08660 and 08860-AB.

Estimation of space use and home range size

We separated the data for each individual into breeding season and nonbreeding season and only included individuals with more than 1000 reported locations within a season. For individuals that were monitored for multiple seasons, we analyzed each season separately and we also used the total available data for each of these individuals for an overall analysis. The breeding season was defined as March–August using the Pennsylvania Bird Atlas breeding guidelines (Pennsylvania Bird Atlas 2024), which included all months where possible breeding was expected. The nonbreeding season was defined as September–February. As there is limited previous documentation regarding home ranges of crows, we included

multiple home range estimators in our analysis to document variability in size of home range estimates and because no estimator has been proven to be a best representation (Walter et al. 2011, 2015). We used 50% and 95% contours to represent core use area and overall size of home range, respectively, for each estimator and all estimators were fit using program R (R Core Team 2022).

We used Brownian bridge movement model (BBMM) based on previous application of BBMM on avian GPS data to determine size of home range (Fischer et al. 2013). We used the *adehabitatHR* package (Calenge and Fortmann 2023) to fit a BBMM for each crow across seasons. A dynamic Brownian bridge movement model (dBBMM) with a maximum time lag of 12 hours was used to calculate home range for each crow using the *move* package (Kranstauber et al. 2023).

Additionally, we used movement-based kernel density estimator (MKDE) because it incorporates time duration between locations and resources available using *adehabitatHR* package (Calenge and Fortmann 2023). Parameters included: maximum time between locations of 12 hours and locations within 50 meters of the previous location were classified as inactive. To prepare the diffusion matrix based on movement through the landscape, we estimated three home ranges: one without covariates (MKDE_{null}), one that included a land cover habitat layer (MKDE_{LC}) with 4 habitat categories, forest, water, developed, and open habitats (Dewitz 2023), and one that depended on elevation (MKDE_{elevation}) with elevation delineated into 200 meter classes (Dewitz and U.S. Geological Survey 2021). We used kernel density estimator with iterative plug-in bandwidth selection (PKDE) due to its ability to process dependent data such as fine scale GPS animal locations (Hall et al. 1995). We used the *amt* package to calculate the PKDE home range for each crow (Signer et al. 2019).

Integrated step selection function

In order to generate habitat layers we obtained landcover from the National Land Cover Database at a 30 meter resolution using the *FedData* package (Dewitz and U.S. Geological Survey 2021; Bocinsky 2024). We reclassified land cover into 4 categories (water, developed, forest, and open) based on previous use of the landscapes by crows equipped with transmitters and functionality of land cover. Elevation, slope, and

aspect were extracted from digital elevation models using the *FedData* package (U.S. Geological Survey 2023; Bocinsky 2024)

We conducted a manual search of landfills and compost facilities on google maps to identify these locations and we digitized an approximate centroid location of each operation for use in measuring distance to the nearest facility. This was the best available method for identifying these locations as neither a spatial layer nor a directory of locations is currently available. Carcass disposal dumpsters are maintained by PGC, and locations are provided to the public for hunter use. Locations of captive cervid facilities with white-tailed deer that tested positive for CWD and the carcass dumpsters were included as one combined covariate layer (hereafter referred to as *risk*), as they are locations where crows may consume or otherwise be exposed to prions responsible for CWD. We obtained primary and secondary road shapefiles from the U.S. Census Bureau TIGER/Line® files using the *tigris* package (U.S. Census Bureau 2022; Walker 2016). We obtained human population density at a 30 meter resolution (Center for International Earth Science Information Network 2018) and we delineated areas with a population density of 2500 persons per square mile or more as populated areas. This population threshold was used by the US Census Bureau in 2010 as the threshold between rural and urban locations.

We used *amt* package (Signer et al. 2019) to fit an integrated step selection function (iSSF). Models for our iSSF incorporate a predictor for step length and covariate values are recorded at the end point of each individual step. For each step present in our data, we generated 4 random steps to provide the comparative available covariate values to those recorded being utilized by the crow. We used Akaike's Information Criteria adjusted for small sample sizes (AICc; Anderson and Burnham 2002) to select models with the most support within our iSSF for each crow. Covariates of interest for our iSSF included: distance to land cover categories, elevation, distance from nearest captive cervid facility or carcass disposal dumpster (*risk*), distance from nearest landfill or compost facility (*waste*), distance to nearest primary or secondary road, and distance from nearest populated area. For our models, we fit 24 unique combinations of covariates. (Supplemental Table 1).

RESULTS

A total of 15 American crows were captured and equipped with a backpack GPS transmitter. Several crows were able to remove their harnesses, and one transmitter stopped recording data shortly after deployment. Eight individuals recorded at least 1,000 locations for a total of 53,521 GPS locations. Six crows have location data for a single season (Table 2.1) and both AMCR007 (Table 2.2) and AMCR011 (Table 2.3) have location data across multiple seasons. Home range estimates for each individual by season were calculated using BBMM, dBBMM, $MKDE_{null}$, $MKDE_{LC}$, $MKDE_{elevation}$, and PKDE (Figures 2.1–2.13).

Size of home range varied between individual crows as well as across season and estimator used for the same individual (Table 2.4). Mean 95% home range size for breeding season for BBMM was 84.40 km² (range: 6.51 – 323.02 km²), for dBBMM was 43.66 km² (range: 3.71 – 214.79 km²), for $MKDE_{null}$ was 56.46 km² (range: 5.05 – 270.9 km²), for $MKDE_{LC}$ was 31.44 km² (range: 2.64 – 144.22 km²), for $MKDE_{elevation}$ was 38.47 km² (range: 4.21 – 184.72 km²), and for PKDE was 30.82 km² (range: 0.76 – 169.17 km²). Mean 95% home range size for nonbreeding season for BBMM was 223.53 km² (range: 100.36 – 346.7 km²), for dBBMM was 33.49 km² (range: 16.07 – 50.90 km²), for $MKDE_{null}$ was 27.02 km² (range: 24.82 – 29.23 km²), for $MKDE_{LC}$ was 17.59 km² (range: 15.15 – 20.03 km²), for $MKDE_{elevation}$ was 33.41 km² (range: 25.66 – 41.16 km²), and for PKDE was 9.87 km² (range: 5.73 – 14.01 km²).

We fit iSSFs to 8 individual crows using the data from the breeding seasons (Table 2.5). The model of best fit for AMCR001 included selection for areas closer to waste, further from water, and with lower elevations. For AMCR002 the model of best fit included selection for areas closer to forest, further from areas of human population, and with lower elevations. For AMCR012 the model of best fit included selection for areas closer to water, closer to risk, and with higher elevations. For AMCR013 the model of

best fit included selection for areas closer to forest, further from roads, and with higher elevations . For AMCR014 the model of best fit included selection for areas closer to water, closer to waste, and with higher elevations. For AMCR015 the model of best fit included selection for areas closer to open habitat and further from waste.

For two individuals there was data collected across multiple seasons and we analyzed data from each season separately as well as collectively for the individual (Table 2.6). For AMCR007 breeding season 1 the model of best fit included selection for areas closer to forest, closer to waste, and with higher elevations whereas for breeding season 2 the model of best fit included selection for areas closer to water, closer to waste, and with higher elevations. For the nonbreeding season the model of best fit for AMCR007 included selection for areas further from water, closer to waste, and with higher elevations whereas for combined across seasons the model of best fit included selection for areas closer to forest, closer to waste, and with higher elevations. For AMCR011 breeding season the model of best fit included selection for areas closer to water, further from waste, and with higher elevations whereas for nonbreeding season the model of best fit included selection for areas closer to water, closer to risk, and with lower elevations. For AMCR011 combined across seasons the model of best fit included selection for closer to water, further from waste, and with higher elevations.

The most common model of best fit included distance to water, distance to waste, and elevation occurring 6 times (Table 2.7). This model was the most common model of best fit, however, individuals differed with both positive and negative relationships with each covariate occurring in these models. Across 13 models of best fit there was the inclusion of both positive and negative relationships associated with distance to waste, distance to water, distance to risk, and elevation. The only covariate to occur in multiple models of best fit and to be selected for in those models was distance to forest. The only covariate that did not occur in at least one model of best fit was distance to road.

DISCUSSION

Our size of home range estimates from crows equipped with GPS transmitters were larger than those from previous VHF studies that used MCP and fixed kernel estimation with least squares cross validation estimators. The methodology and technical limitations of these VHF studies likely resulted in data that underrepresented the areas used by individuals. Sullivan and Dinsmore (1992) used a mixture of location data from visually tracking individuals and locations from VHF transmitters while Yaremchuk et al. (2004b) used VHF tracking to find individuals and then recorded locations based on visual observations once located. Large time gaps (days to weeks) between recorded locations and the need for trackers to locate individuals increases the proportion of time that the location of the crows was unknown likely resulting in a less complete representation of their space use. In contrast to VHF studies, average 95% home range size of 235 km² using GPS tracking data and MCP was larger than our estimates (Taff et al. 2016). For GPS data, polygon-based home range estimators have been shown to provide less accurate representations than kernel density-based estimators and estimators with a temporal component (Walter et al. 2015). In addition to the difference in the home range estimators used, Taff et al. (2016) consisted of less frequent recorded locations (9 per day) and smaller total overall data set (2,147 locations) despite having a similar sample size of individuals (n=7 crows) compared to our data (10-minute locations, 53,521 locations, n=8 crows). Biotic and abiotic factors influence home range size at a regional scale, landscape scale, temporal scale, and individual scale and the progression of improved data collection and improved tools for estimation enable us to fit increasingly more representative home range estimations.

Although there has been limited previous GPS transmitter data collection for crows, the advancements in transmitter technology have enabled data collection for other avian species. The common raven (*Corvus corax*), which also belongs to the family Corvidae, were found to have an average home range of 337.53 km² during their non-breeding dispersal stage estimated using MCP (Loretto et al. 2016). The study of larger avian scavengers has been less restricted by transmitter size as they could be outfitted with heavier transmitters. Black vultures (*Coragyps atratus*) were found to have an average size

of home range of 467 km² calculated by BBMM and 2545 km² by a kernel density estimator (Fischer et al. 2013). Turkey vultures (*Cathartes aura*) were found to have an average size of home range of 2854 km² calculated by BBMM and 13011 km² by a kernel density estimator (Fischer et al. 2013). The technological advancements of GPS transmitters for avian species are valuable because this data can be leveraged to understand the resource selection of birds within their environments.

In addition to the estimation of home range size it is important to understand the underlying drivers of space use. Avian scavengers have been shown to select for locations of consistent food availability, particularly anthropogenic sources, and retain a knowledge of these locations for repeated use (Monsarrat et al. 2013; Loretto et al. 2016). Three resource groups related to available food resources in our models included: (1) human populated areas, (2) waste, and (3) risk and all three of these covariates were included in the model of best fit for at least one individual with waste occurring the most frequently. Given our relatively small sample size, the importance of all 3 of these covariates in some form indicates that food resources as a category are important but there is not a singular food resource that drives crow space use across all individuals. At a landscape scale, the distribution and abundance of these 3 resource groups is not equal and individuals may be selecting for the food resource most available to them at a local scale. This is of particular interest regarding the risk resource group (carcass dumpsters, captive cervid facilities) because a preference for this group would indicate that an individual may visit repeatedly that could result in repeated exposure to infectious prions or a possible movement pathway for disease.

RESEARCH IMPLICATIONS

Deploying GPS transmitters on crows was challenging but data collected in this study is the largest such dataset of crow GPS transmitter locations to date. Space use estimates have been very different from VHF and GPS transmitter technology and we documented the limitations of previously used datasets. We did not observe long range dispersal or migration for any of our study crows, both of which have been previously documented in some individuals so additional studies with larger sample sizes of captured

crows are warranted. A larger sample size would likely capture these aspects of crow space use for some individuals. We documented that crows selected for areas that place them at risk of exposure to zoonotic diseases (human landscape, landfills) as well as risk of exposure to prion diseases (carcass dumpsters and captive cervid facilities). Avian species have been documented to transport plant materials and disease, but the role they play in transmission of infectious prions was relatively unknown prior to our study. Additional research on crow space use and testing/detection of prions in crows is warranted to continue to build our understanding of avian spatial ecology in relation to disease transmission and spread.

ACKNOWLEDGEMENTS

The U.S. Department of Agriculture-Animal Plant and Health Inspection Service-Wildlife Services provided funding for this research. The Pennsylvania Game Commission provided specific information regarding CWD within our study area and provided access to locations for crow capture. Margaret Brittingham provided her invaluable expertise as a master bander for this project. This project would not have been possible without the following individuals who devoted many hours to assist with crow capture: D. Pearce, A. Fameli, J. Edson, A. Cruz, K. Smelter, K. Witmer, E. Miller, J. Yacabucci, K. Lamp, R. Walters, and J. Hoy-Petersen. Any opinions, findings, conclusions, or recommendations expressed in this publication are those of the authors and should not be construed to represent any official USDA or U.S. Government determination or policy. Any use of trade, firm, or product names is for descriptive purposes only and does not imply endorsement by the U.S. Government.

REFERENCES

- Anderson, D. R., and K. P. Burnham. 2002. Avoiding pitfalls when using information-theoretic methods. *The Journal of Wildlife Management* 66(3):912–918.
- Bocinsky, R. K. 2024. FedData: Functions to Automate Downloading Geospatial Data Available from Several Federated Data Sources. R package version 4.0.1.
- Caffrey, C. 2002. Catching crows. *North American Bird Bander* 26(4):137–145.
- Calenge, C., and S. Fortmann-Roe. 2023. adehabitatHR: home range estimation. R package version 0.4.21.
- Center for International Earth Science Information Network - CIESIN - Columbia University. 2018. Gridded population of the world, version 4 (gpwv4): Population density, revision 11, Socioeconomic Data and Applications Center (SEDAC).
- de la Fuente, J., A. Estrada-Peña, A. Cabezas-Cruz, and R. Brey. 2015. Flying ticks: anciently evolved associations that constitute a risk of infectious disease spread. *Parasites Vectors* 8:538.
- Dewitz, J., and U.S. Geological Survey, 2021, National Land Cover Database (NLCD) 2019 Products (ver. 3.0, February 2024): U.S. Geological Survey data release.
- Fischer, J. W., W. D. Walter, and M. L. Avery. (2013). Brownian bridge movement models to characterize birds' home ranges. *The Condor* 115(2): 298–305.
- Gaidet, N., J. Cappelle, J. Y. Takekawa, D. J. Prosser, S. A. Iverson, D. C. Douglas, and S. H. Newman. 2010. Potential spread of highly pathogenic avian influenza H5N1 by wildfowl: dispersal ranges and rates determined from large-scale satellite telemetry. *Journal of Applied Ecology* 47(5): 1147–1157
- Garmyn, A, P. Van Rooij, F. Pasmans, T. Hellebuyck, W. Van Den Broeck, F. Haesebrouck, and A. Martel. 2012. Waterfowl: Potential Environmental Reservoirs of the Chytrid Fungus *Batrachochytrium dendrobatidis*. *PLoS ONE* 7(4): e35038.

- Grove, D. M., A. M. Zajac, J. Spahr, R. B. Duncan, and J. M. Sleeman. 2005. Combined infection by avian poxvirus and *Collyriclum faba* in an American crow (*Corvus brachyrhynchos*). *Journal of Zoo and Wildlife Medicine* 36(1):111–114.
- Hall, P., S. N. Lahiri, and Y. K. Truong. 1995. On bandwidth choice for density estimation with dependent data. *The Annals of Statistics* 23(6):2241–2263.
- Hanlon, S. M, J. R. Henson, and J. L. Kerby. 2017. Detection of amphibian chytrid fungus on waterfowl integument in natural settings. *Diseases of Aquatic Organisms* 126:71-74.
- Kalmbach, E. R., & S. E. Aldous. 1940. Winter banding of oklahoma crows. *The Wilson Bulletin* 52(3):198–206.
- Karl, B. J., and M. N. Clout. 1987. An improved radio transmitter harness with a weak link to prevent snagging. *Journal of field Ornithology* 58(1):73–77.
- Kranstauber, B., M. Smolla, and A. K. Scharf. 2023. Move: Visualizing and analyzing animal track data. R package version 4.2.4.
- Loretto, M., R. Schuster, and T. Bugnyar. 2016. GPS tracking of non-breeding ravens reveals the importance of anthropogenic food sources during their dispersal in the Eastern Alps. *Current Zoology* 62(4):337–344,
- Malewski, T., B. Brzezińska, B. Lassaad, and T. Oszako. 2019. Role of avian vectors in the spread of *Phytophthora* species in Poland. *European Journal of Plant Pathology* 155.
- Monsarrat, S., S. Benhamou, F. Sarrazin, C. Bessa-Gomes, W. Bouten, and O. Duriez. 2013. How predictability of feeding patches affects home range and foraging habitat selection in avian social scavengers?. *PLoS One* 8(1):e53077.
- Nathan, R., and H. C. Muller-Landau. 2000. Spatial patterns of seed dispersal, their determinants and consequences for recruitment. *Trends in ecology & evolution* 15(7):278–285
- Neatherlin, E. A., J. M. Marzluff, and Peterson. 2004. Responses of american crow populations to campgrounds in remote native forest landscapes. *Journal of Wildlife Management* 68(3):708–718.

- Padilla, D. P., A. González-Castro, and M. Nogales. 2012. Significance and extent of secondary seed dispersal by predatory birds on oceanic islands: the case of the Canary archipelago. *Journal of Ecology* 100(2):416–427.
- Pennsylvania Bird Atlas. 2024. Pennsylvania Bird Atlas 3 Breeding Guidelines Chart. < https://is-ebird-wordpress-prod-s3.s3.amazonaws.com/wp-content/uploads/sites/97/2024/02/PA-Bird-Atlas-Breeding-Guidelines-Chart_v1.1.pdf> Accessed 30 Oct 2024.
- Pennsylvania Game Commission. 2020. Pennsylvania chronic wasting disease response plan. <<https://www.pgc.pa.gov/Wildlife/WildlifeHealth/Documents/Final%20CWD%20Response%20Plan%20July%202020.pdf>>. Accessed 30 Oct 2024.
- Prisockck, A. M., B. S. Dorr, and J. C. Cumbee. 2012. Modification of net configurations of the coda netlauncher® to enhance bird capture. *Human-Wildlife Interactions* 6(2):237–244.
- Proctor, V. W. 1968. Long-distance dispersal of seeds by retention in digestive tract of birds. *Science* 160(3825):321–322.
- R Core Team. 2022. R: A language and environment for statistical computing. version 4.2.1. R Foundation for Statistical Computing, Vienna, Austria.
- Sen, K., V. Shepherd, T. Berglund, A. Quintana, S. Puim, R. Tadmori, J. T. R, L. Khalil, and M. A. Soares. 2020. American crows as carriers of extra intestinal pathogenic *E. Coli* and avian pathogenic-like *E. Coli* and their potential impact on a constructed wetland. *Microorganisms* 8(10):1595.
- Signer, J., J. Fieberg, and T. Avgar. 2019. Animal movement tools (amt): R package for managing tracking data and conducting habitat selection analyses. R package version 0.2.2.0. *Ecology and Evolution* 9(2):880–890.

- Sullivan, B. D., and J. J. Dinsmore. 1992. Home range and foraging habitat of American crows, *Corvus brachyrhynchos*, in a waterfowl breeding area in manitoba. *The Canadian field-naturalist* 106(2): 181–184.
- Taff, C. C., A. M. Weis, S. Wheeler, M. G. Hinton, B. C. Weimer, C. M. Barker, M. Jones, R. Logsdon, W. A. Smith, W. M. Boyce et al. 2016. Influence of host ecology and behavior on *Campylobacter jejuni* prevalence and environmental contamination risk in a synanthropic wild bird species. *Applied Environmental Microbiology* 82(15):4811–4820.
- Townsend, A. K., B. Frett, A. Mcgarvey, and C. C. Taff. 2018. Where do winter crows go? Characterizing partial migration of American crows with satellite telemetry, stable isotopes, and molecular markers. *The Auk: Ornithological Advances* 135(4):964–974.
- U.S. Geological Survey. 2023., 3D elevation program 1-meter resolution digital elevation model.<
<https://www.usgs.gov/the-national-map-data-delivery>> Accessed 30 Oct 2024.
- U.S. Census Bureau. 2022. U.S. Census 2022 tiger/line® files [machine-readable data files]. U.S. Census Bureau , Washington , D.C.
- Vercauteren, K. C., J. L. Pilon, P. B. Nash, G. E. Phillips, and J. W. Fischer. 2012. Prion remains infectious after passage through digestive system of american crows (*Corvus brachyrhynchos*). *PLoS One* 7(10):e45774.
- Walker, K. E.. 2016. tigris: An R package to access and work with geographic data from the US Census Bureau. R package version 2.1. *The R Journal* 8(2):231–242.
- Walter, W. D., J. W. Fischer, S. Baruch-Mordo, and K. C. Vercauteren. 2011. What is the proper method to delineate home range of an animal using today’s advanced gps telemetry systems: The initial step. *Modern telemetry* 68.
- Walter, W. D., D. P. Onorato, and J. W. Fischer. 2015. Is there a single best estimator? Selection of home range estimators using area-under-the-curve. *Movement Ecology* 3(1):10.

- Wilcox, B. R., M. J. Yabsley, A. E. Ellis, D. E. Stallknecht, and S. E. Gibbs. 2007. West Nile virus antibody prevalence in American crows (*Corvus brachyrhynchos*) and fish crows (*Corvus ossifragus*) in Georgia, USA. *Avian Diseases* 51(1):125–128.
- Williams, E. S., and S. Young. 1980. Chronic wasting disease of captive mule deer: A spongiform encephalopathy. *Journal of Wildlife Diseases* 16(1):89–98.
- Withey, J. C., and J. M. Marzluff. 2008. Multi-scale use of lands providing anthropogenic resources by American crows in an urbanizing landscape. *Landscape Ecology* 24(2):281–293.
- Yaremych, S. A., R. E. Warner, P. C. Mankin, J. D. Brawn, A. Raim, and R. Novak. 2004a. West Nile virus and high death rate in American crows. *Emergent Infectious Diseases* 10(4):709–711.
- Yaremych, S. A., R. J. Novak, A. J. Raim, P. C. Mankin, and R. E. Warner. 2004b. Home range and habitat use by American crows in relation to transmission of West Nile virus. *The Wilson Bulletin* 116(3):232–239.

Table 2.1 Breeding season home range estimate size for American crows (*Corvus brachyrhynchos*) in Pennsylvania, USA, 2023-2024. Home range estimators were Brownian bridge movement model (BBMM), dynamic Brownian bridge movement model (dBBMM), movement-based kernel density estimation (MKDE) with associated habitat layer, and kernel density estimation with plug-in bandwidth selection (PKDE).

Individual ID	Number of locations	Home range isopleth (area in km ²)				Estimator
		50%	80%	90%	95%	
AMCR001	1149	10.64	77.13	156.99	243.12	BBMM
		0.57	11.64	43.16	101.74	dBBMM
		2.46	22.42	64.53	124.98	MKDE _{null}
		0.48	7.75	30.33	75.60	MKDE _{LC}
		0.56	12.57	44.46	89.45	MKDE _{elevation}
		9.31	95.91	95.91	169.17	PKDE
AMCR002	8890	0.82	5.07	9.37	14.70	BBMM
		0.31	1.71	4.03	7.08	dBBMM
		0.54	3.34	7.52	12.87	MKDE _{null}
		0.18	1.25	2.94	5.22	MKDE _{LC}
		0.24	1.56	3.51	5.95	MKDE _{elevation}
		0.19	1.12	1.12	1.89	PKDE
AMCR007 -1	6980	0.51	3.04	7.21	12.95	BBMM
		0.27	1.65	5.28	14.62	dBBMM
		0.52	2.44	5.70	10.93	MKDE _{null}
		0.24	1.23	3.24	7.65	MKDE _{LC}
		0.31	1.42	2.91	5.70	MKDE _{elevation}
		0.12	0.85	0.85	1.45	PKDE
AMCR007 -2	1141	7.69	27.03	47.03	70.53	BBMM
		2.26	8.65	16.28	28.09	dBBMM
		4.67	14.60	24.21	35.28	MKDE _{null}
		3.64	11.60	19.63	29.14	MKDE _{LC}
		2.29	7.30	11.83	17.14	MKDE _{elevation}
		0.69	4.43	4.43	6.86	PKDE
AMCR011	7349	1.19	8.95	15.91	23.32	BBMM
		0.47	2.52	6.70	11.65	dBBMM
		0.58	3.40	7.95	12.92	MKDE _{null}
		0.29	1.46	4.06	6.78	MKDE _{LC}
		0.53	2.99	7.26	11.86	MKDE _{elevation}
		0.29	1.46	1.46	2.30	PKDE
AMCR012	5313	21.25	96.92	191.77	323.02	BBMM

		0.27	15.44	70.39	214.79	dBBMM
		1.67	25.81	102.33	270.90	MKDE _{null}
		0.30	10.47	37.87	144.22	MKDE _{LC}
		0.88	10.94	46.87	184.72	MKDE _{elevation}
		-	23.72	23.72	91.52	PKDE
AMCR013	8646	0.88	6.72	14.18	22.81	BBMM
		0.09	0.53	1.27	3.71	dBBMM
		0.25	0.74	1.89	5.05	MKDE _{null}
		0.09	0.23	0.73	2.64	MKDE _{LC}
		0.22	0.32	1.22	4.21	MKDE _{elevation}
		0.06	0.69	0.69	1.23	PKDE
AMCR014	4031	2.29	12.70	23.52	36.06	BBMM
		0.39	1.88	3.94	7.03	dBBMM
		1.33	6.58	14.19	25.00	MKDE _{null}
		0.46	2.05	4.54	8.78	MKDE _{LC}
		1.21	5.82	12.41	21.52	MKDE _{elevation}
		0.14	1.19	1.19	2.17	PKDE
AMCR015	5965	0.24	2.47	6.51	13.09	BBMM
		0.09	0.44	1.27	4.28	dBBMM
		0.23	1.49	4.84	10.26	MKDE _{null}
		0.02	0.34	0.98	2.92	MKDE _{LC}
		0.11	0.80	2.59	5.64	MKDE _{elevation}
		0.06	0.41	0.41	0.76	PKDE

Table 2.2 Home range estimate size by season for an American crow (*Corvus brachyrhynchos*) with data for two breeding seasons, a nonbreeding season, and the combined data of all three seasons in Pennsylvania, USA, 2023-2024. Home range estimators were Brownian bridge movement model(BBMM), dynamic Brownian bridge movement model (dBBMM), movement-based kernel density estimation (MKDE) with associated habitat layer, and kernel density estimation with plug-in bandwidth selection (PKDE).

Individual ID	Season	Number of locations	Home range isopleth (area in km ²)				Estimator
			50%	80%	90%	95%	
AMCR007	Breeding 1	6980	0.51	3.04	7.21	12.95	BBMM
			0.27	1.65	5.28	14.62	dBBMM
			0.52	2.44	5.70	10.93	MKDE _{null}
			0.24	1.23	3.24	7.65	MKDE _{LC}
			0.31	1.42	2.91	5.70	MKDE _{elevation}
			0.12	0.85	0.85	1.45	PKDE
	Nonbreeding	1040	21.49	99.66	206.45	346.70	BBMM
			0.87	3.79	8.40	16.07	dBBMM
			2.52	9.50	16.59	24.82	MKDE _{null}
			1.40	6.70	12.88	20.03	MKDE _{LC}
			1.90	10.87	24.05	41.16	MKDE _{elevation}
			0.33	2.68	2.68	5.73	PKDE
	Breeding 2	1141	7.69	27.03	47.03	70.53	BBMM
			2.26	8.65	16.28	28.09	dBBMM
			4.67	14.60	24.21	35.28	MKDE _{null}
			3.64	11.60	19.63	29.14	MKDE _{LC}
			2.29	7.30	11.83	17.14	MKDE _{elevation}
			0.69	4.43	4.43	6.86	PKDE
	Combined	9161	5.17	27.27	58.00	107.22	BBMM
			0.91	4.88	12.93	25.79	dBBMM
			1.71	6.68	12.52	19.86	MKDE _{null}
0.57			3.58	8.18	14.49	MKDE _{LC}	
1.06			4.63	8.85	14.67	MKDE _{elevation}	
0.17			1.78	1.78	3.33	PKDE	

Table 2.3 Home range estimate size by season for an American crow (*Corvus brachyrhynchos*) with data from one breeding season, one nonbreeding season, and the combined data of these seasons in Pennsylvania, USA, 2023-2024. Home range estimators were Brownian bridge movement model (BBMM), dynamic Brownian bridge movement model (dBBMM), movement-based kernel density estimation (MKDE) with associated habitat layer, and kernel density estimation with plug-in bandwidth selection (PKDE).

Individual ID	Season	Number of locations	Home range isopleth (area in km ²)				Estimator
			50%	80%	90%	95%	
AMCR011	Nonbreeding	3089	9.18	39.68	67.85	100.36	BBMM
			0.74	4.82	19.75	50.90	dBBMM
			1.10	5.13	13.56	29.23	MKDE _{null}
			0.51	2.59	6.38	15.15	MKDE _{LC}
			0.98	4.62	11.03	25.66	MKDE _{elevation}
			0.69	6.68	6.68	14.01	PKDE
	Breeding	7349	1.19	8.95	15.91	23.32	BBMM
			0.47	2.52	6.70	11.65	dBBMM
			0.58	3.40	7.95	12.92	MKDE _{null}
			0.29	1.46	4.06	6.78	MKDE _{LC}
			0.53	2.99	7.26	11.86	MKDE _{elevation}
			0.29	1.46	1.46	2.30	PKDE
	Combined	10438	3.25	18.15	32.13	49.30	BBMM
			0.56	3.31	8.95	18.32	dBBMM
			0.76	4.44	10.67	20.72	MKDE _{null}
			0.43	2.21	5.84	10.18	MKDE _{LC}
			0.69	3.91	9.76	17.63	MKDE _{elevation}
			0.39	2.75	2.75	5.46	PKDE

Table 2.4 Minimum, maximum, and average American crow (*Corvus brachyrhynchos*) home range estimates for breeding and nonbreeding seasons in Pennsylvania, USA, 2023-2024. Home range estimators were Brownian bridge movement model (BBMM), dynamic Brownian bridge model (dBBMM), movement-based kernel density estimation (MKDE) with associated habitat layer, and kernel density estimation with plug-in bandwidth selection (PKDE).

Season	Estimator	50% Home Range (area in km ²)			95% Home Range (area in km ²)		
		Min	Max	Average	Min	Max	Average
Breeding	BBMM	0.24	21.25	5.06	6.51	323.02	84.40
	dBBMM	0.09	2.26	0.52	3.71	214.79	43.66
	MKDEnull	0.23	4.67	1.36	5.05	270.90	56.46
	MKDELC	0.02	3.64	0.63	2.64	144.22	31.44
	MKDEelevation	0.11	2.29	0.71	4.21	184.72	38.47
	PKDE	-	9.31	-	0.76	169.17	30.82
Non-breeding	BBMM	9.18	21.49	15.34	100.36	346.70	223.53
	dBBMM	0.74	0.87	0.81	16.07	50.90	33.49
	MKDEnull	1.10	2.52	1.81	24.82	29.23	27.02
	MKDELC	0.51	1.40	0.95	15.15	20.03	17.59
	MKDEelevation	0.98	1.90	1.44	25.66	41.16	33.41
	PKDE	0.33	0.69	0.51	5.73	14.01	9.87

Table 2.5 Integrated step selection function model of best fit for individual American crows (*Corvus brachyrhynchos*) during the breeding season with coefficient, exponential coefficient, and upper and lower 95% confidence intervals (CI) for each model element. Pennsylvania, USA, 2023.

Individual ID	Variable	Coefficient	exp(Coefficient)	95% CI	
AMCR001	water	4.790E-04	1.000E+00	3.071E-04	6.509E-04
	waste	-1.522E-04	9.998E-01	-2.473E-04	-5.712E-05
	elevation	-1.115E-02	9.889E-01	-1.468E-02	-7.619E-03
	step length	8.300E-05	1.000E+00	6.007E-06	1.600E-04
AMCR002	forest	-7.288E-03	9.927E-01	-8.544E-03	-0.006
	h_pop	9.616E-04	1.001E+00	8.022E-04	0.001
	elevation	-1.122E-02	9.888E-01	-1.232E-02	-0.010
	step length	1.326E-04	1.000E+00	2.248E-05	2.428E-04
AMCR007 -1	forest	-4.198E-03	9.958E-01	-0.005	-0.004
	waste	-1.021E-03	9.990E-01	-1.200E-03	-8.420E-04
	elevation	2.516E-02	1.025E+00	0.021	0.029
	step length	9.774E-05	1.000E+00	-2.994E-05	2.254E-04
AMCR007 -2	water	-1.139E-03	9.989E-01	-0.002	-0.001
	waste	-2.017E-03	9.980E-01	-0.003	-0.001
	elevation	6.320E-02	1.065E+00	0.046	0.080
	step-length	5.640E-04	1.001E+00	2.377E-04	0.001
AMCR011	water	-1.816E-03	9.982E-01	1.996E-03	-1.636E-03
	waste	7.139E-04	1.001E+00	5.722E-04	8.557E-04
	elevation	5.256E-03	1.005E+00	0.004	0.007
	step length	2.823E-04	1.000E+00	1.798E-04	3.848E-04
AMCR012	water	-5.510E-04	9.994E-01	-6.537E-04	-4.482E-04
	risk	-6.825E-04	9.993E-01	-7.464E-04	-6.187E-04
	elevation	1.482E-03	1.001E+00	0.001	0.002
	step length	1.936E-04	1.000E+00	1.506E-04	2.365E-04
AMCR013	forest	-2.185E-03	9.978E-01	-2.436E-03	-1.934E-03
	roads	3.337E-03	1.003E+00	0.003	0.004
	elevation	2.195E-02	1.022E+00	0.018	0.026
	step length	3.641E-04	1.000E+00	2.896E-04	4.386E-04
AMCR014	water	-2.227E-03	9.978E-01	-2.437E-03	-2.017E-03

	waste	-2.015E-03	9.980E-01	-2.228E-03	-1.803E-03
	elevation	1.966E-02	1.020E+00	0.014	0.025
	step length	8.691E-04	1.001E+00	7.340E-04	1.004E-03
AMCR015	open	-5.149E-03	9.949E-01	-0.006	-0.005
	waste	3.811E-04	1.000E+00	2.173E-04	5.449E-04
	step length	1.538E-05	1.000E+00	-1.275E-04	1.583E-04

Table 2.6 Integrated step selection function model of best fit for individuals with multiple seasons of data collected with the coefficient, exponential coefficient, and upper and lower 95% confidence intervals (CI) for each model element. Pennsylvania, USA, 2023-2024.

Individual ID	Season	Variable	Coefficient	exp(Coefficient)	95% CI	
AMCR007	Breeding 1	forest	-4.198E-03	9.958E-01	-0.005	-0.004
		waste	-1.021E-03	9.990E-01	-1.200E-03	-8.420E-04
		elevation	2.516E-02	1.025E+00	0.021	0.029
		step length	9.774E-05	1.000E+00	-2.994E-05	2.254E-04
AMCR007	Breeding 2	water	-1.139E-03	9.989E-01	-0.002	-0.001
		waste	-2.017E-03	9.980E-01	-0.003	-0.001
		elevation	6.320E-02	1.065E+00	0.046	0.080
		step-length	5.640E-04	1.001E+00	2.377E-04	0.001
AMCR007	Nonbreeding	water	1.308E-03	1.001E+00	0.001	0.002
		waste	-9.797E-04	9.990E-01	-1.443E-03	-5.165E-04
		elevation	2.201E-02	1.022E+00	0.007	0.037
		step length	-1.689E-04	9.998E-01	-4.867E-04	1.488E-04
AMCR007	Combined	forest	-3.626E-03	9.964E-01	-4.159E-03	-3.093E-03
		waste	-1.115E-03	9.989E-01	-1.274E-03	-9.550E-04
		elevation	2.899E-02	1.029E+00	2.506E-02	3.292E-02
		step length	5.211E-05	1.000E+00	-5.998E-05	1.642E-04
AMCR011	Breeding	water	-1.816E-03	9.982E-01	1.996E-03	-1.636E-03
		waste	7.139E-04	1.001E+00	5.722E-04	8.557E-04
		elevation	5.256E-03	1.005E+00	0.004	0.007
		step length	2.823E-04	1.000E+00	1.798E-04	3.848E-04
AMCR011	Nonbreeding	water	-9.197E-04	9.991E-01	-1.094E-03	-7.452E-04
		risk	-2.477E-04	9.998E-01	-3.586E-04	-1.368E-04
		elevation	-5.870E-03	9.941E-01	-8.431E-03	-3.309E-03
		step length	1.262E-04	1.000E+00	3.688E-05	2.155E-04
AMCR011	Combined	water	-1.444E-03	9.986E-01	-1.570E-03	-1.319E-03
		waste	4.024E-04	1.000E+00	3.107E-04	4.941E-04
		elevation	2.711E-03	1.003E+00	1.584E-03	3.838E-03
		step length	1.578E-04	1.000E+00	8.709E-05	2.284E-04

Table 2.7 Integrated step selection functions models for American crows (*Corvus brachyrhynchos*) for each season (Breeding, Nonbreeding, Combined) in Pennsylvania, USA, 2023-2024 using Akaike information criterion (AICc). Number of parameters in the model (K), change in corrected Akaike information criterion from the lowest AICc ($\Delta AICc$), and AICc model weights ($AICc\omega$) were used to determine top model and strength of competing models. Covariates included: distance to the nearest water (water), distance to nearest forest (forest), distance to open (open), distance to nearest human population of 2500 people per square mile (h_pop), distance to nearest landfill or compost facility (waste), distance to the nearest carcass disposal dumpster or positive captive facility (risk), distance to the nearest primary or secondary road (road), and elevation in meters (elevation). All models also incorporated step length as a model element.

Individual ID	Season	Model Elements	K	AICc	$\Delta AICc$	$AICc\omega$
AMCR001	Breeding	water+waste+elevation	4	3535.49	0.00	0.951
		water+risk+elevation	4	3542.74	7.25	0.025
AMCR002	Breeding	forest+h_pop+elevation	4	26150.39	0.00	1.000
		open+h_pop+elevation	4	26208.76	58.37	0.000
AMCR007	Breeding 1	forest+waste+elevation	4	19256.95	0.00	1.000
		forest+road+elevation	4	19327.08	70.13	0.000
AMCR007	Nonbreeding	water+waste+elevation	4	1518.51	0.00	0.971
		water+waste	3	1526.27	7.76	0.020
AMCR007	Breeding 2	water+waste+elevation	4	1084.81	0.00	0.628
		forest+waste+elevation	4	1086.06	1.25	0.336
		open+waste+elevation	4	1090.54	5.74	0.036
AMCR007	Combined	forest+waste+elevation	4	19256.95	0.00	1.000
		forest+road+elevation	4	19327.08	70.13	0.000
AMCR011	Nonbreeding	water+risk+elevation	4	7914.80	0.00	0.998
		water+waste+elevation	4	7927.84	13.05	0.001
AMCR011	Breeding	water+waste+elevation	4	20837.49	0.00	1.000
		forest+waste	3	20873.30	35.82	0.000
AMCR011	Combined	water+waste+elevation	4	3535.49	0.00	0.951

		water+risk+elevation	4	3542.74	7.25	0.025
AMCR012	Breeding	water+risk+elevation	4	14315.97	0.00	1.000
		water+risk	3	14332.18	16.21	0.000
AMCR013	Breeding	forest+road+elevation	4	25129.14	0.00	1.000
		forest+road	3	25258.06	128.92	0.000
AMCR014	Breeding	water+waste+elevation	4	9781.01	0.00	1.000
		water+waste	3	9826.10	45.09	0.000
AMCR015	Breeding	open+waste	3	15735.57	0.00	0.577
		open+waste+elevation	4	15736.33	0.76	0.395
		water+waste+elevation	4	15741.63	6.06	0.028

Figure 2.1 A) Breeding season GPS locations for AMCR001 in Pennsylvania, USA, 2023. Estimators of home range included: B) Brownian bridge movement model, C) dynamic Brownian bridge movement model, D) movement-based kernel density with null habitat, E) movement-based kernel density estimator with 4 land cover categories (water, developed, forest, open), F) movement-based kernel density with elevation, G) kernel density estimator with plug-in bandwidth selection. Isopleths are 50% (red), 80% (orange), 90% (yellow), and 95% (green).

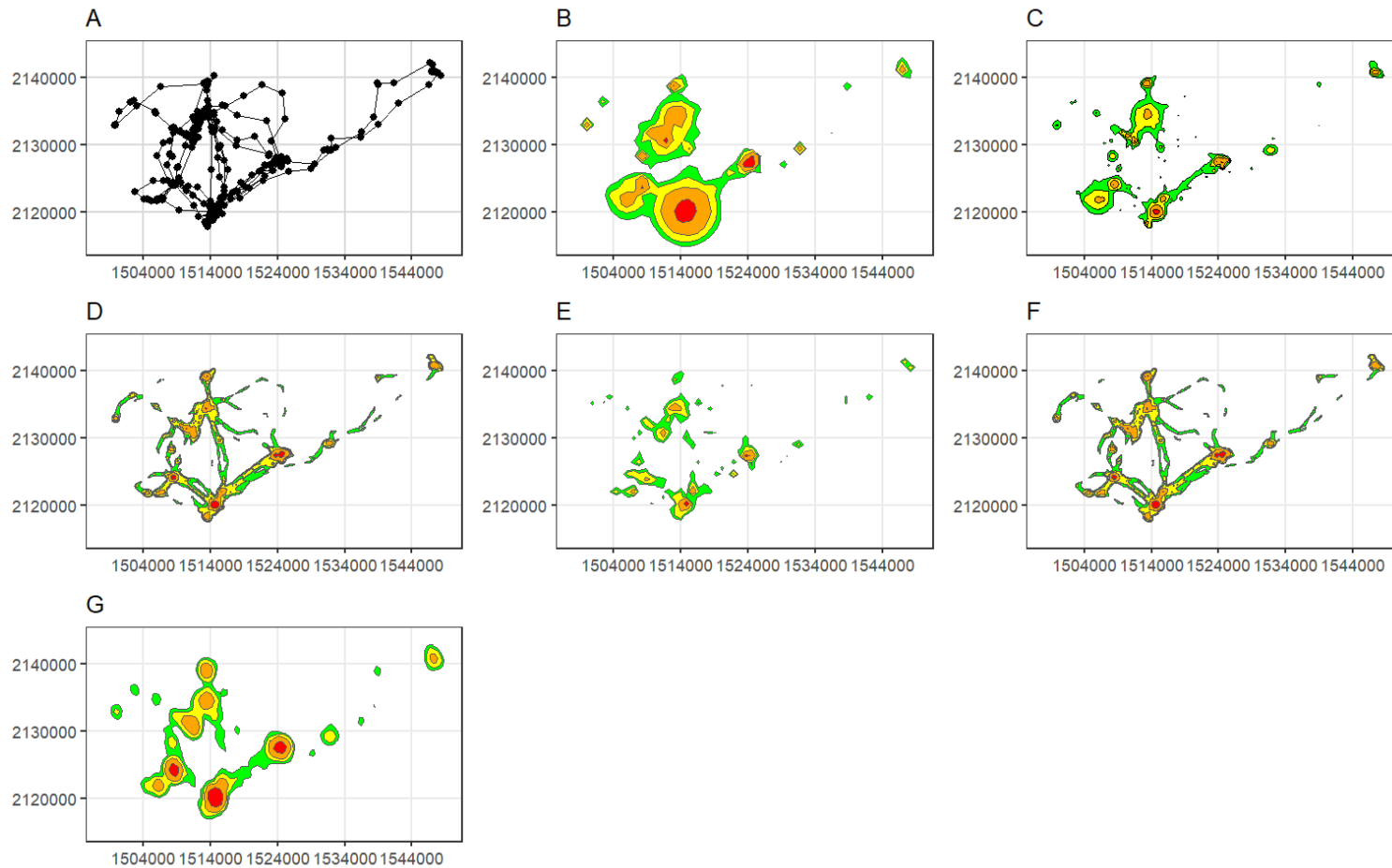


Figure 2.2 A) Breeding season GPS locations for AMCR002 in Pennsylvania, USA, 2023. Estimators of home range included: B) Brownian bridge movement model, C) dynamic Brownian bridge movement model, D) movement-based kernel density with null habitat, E) movement-based kernel density estimator with 4 land cover categories (water, developed, forest, open), F) movement-based kernel density with elevation, G) kernel density estimator with plug-in bandwidth selection. Isopleths are 50% (red), 80% (orange), 90% (yellow), and 95% (green).

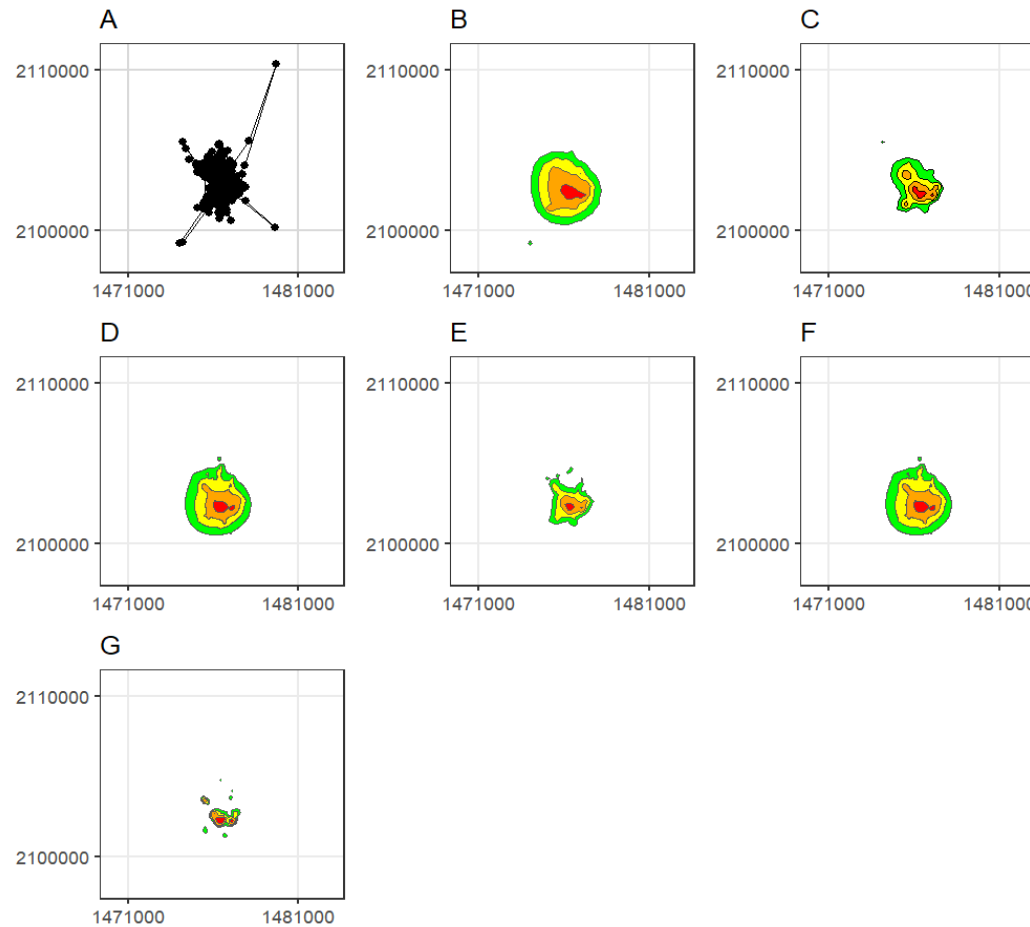


Figure 2.3 A) Breeding season GPS locations for AMCR007 in Pennsylvania, USA, 2023. Estimators of home range included: B) Brownian bridge movement model, C) dynamic Brownian bridge movement model, D) movement-based kernel density with null habitat, E) movement-based kernel density estimator with 4 land cover categories (water, developed, forest, open), F) movement-based kernel density with elevation, G) kernel density estimator with plug-in bandwidth selection. Isopleths are 50% (red), 80% (orange), 90% (yellow), and 95% (green).

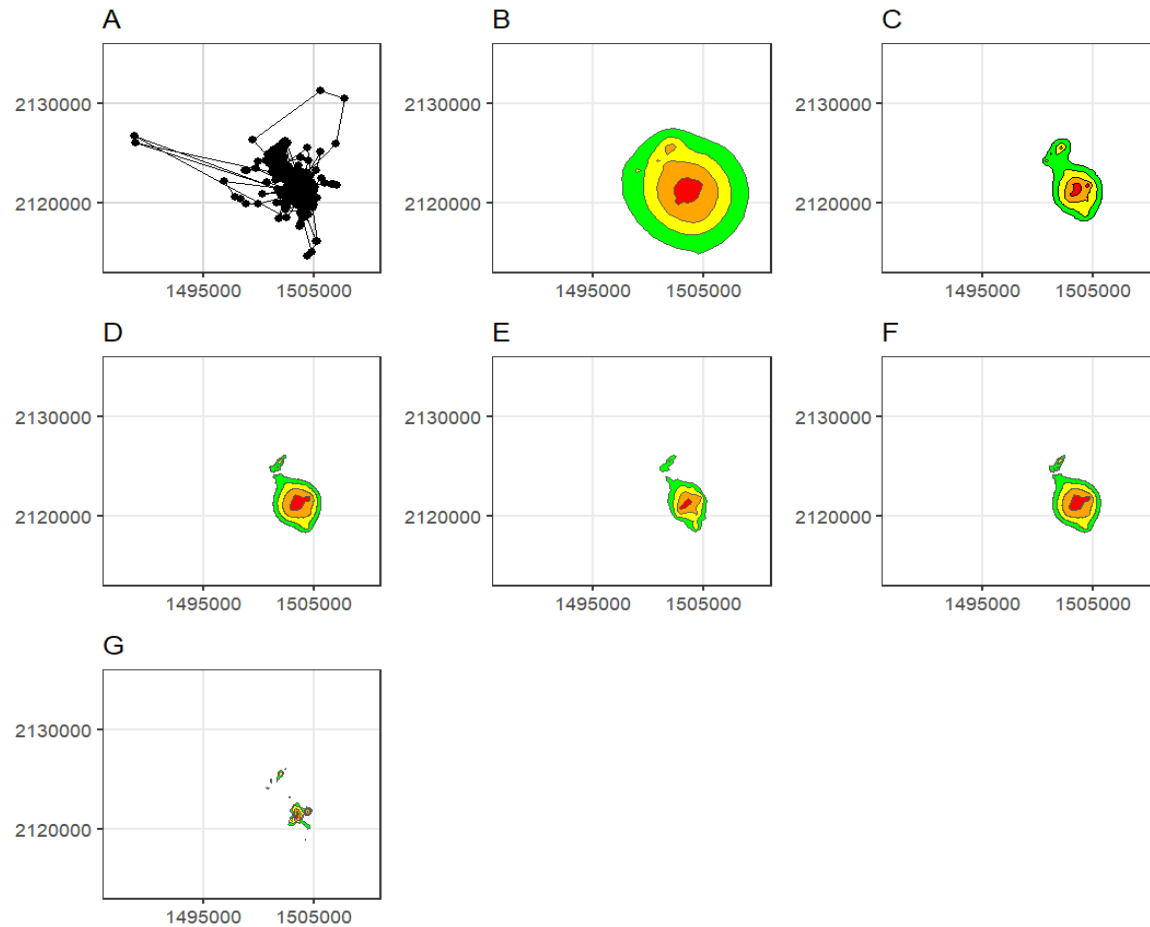


Figure 2.4 A) Nonbreeding season GPS locations for AMCR007 in Pennsylvania, USA, 2023-2024. Estimators of home range included: B) Brownian bridge movement model, C) dynamic Brownian bridge movement model, D) movement-based kernel density with null habitat, E) movement-based kernel density estimator with 4 land cover categories (water, developed, forest, open), F) movement-based kernel density with elevation, G) kernel density estimator with plug-in bandwidth selection. Isopleths are 50% (red), 80% (orange), 90% (yellow), and 95% (green).

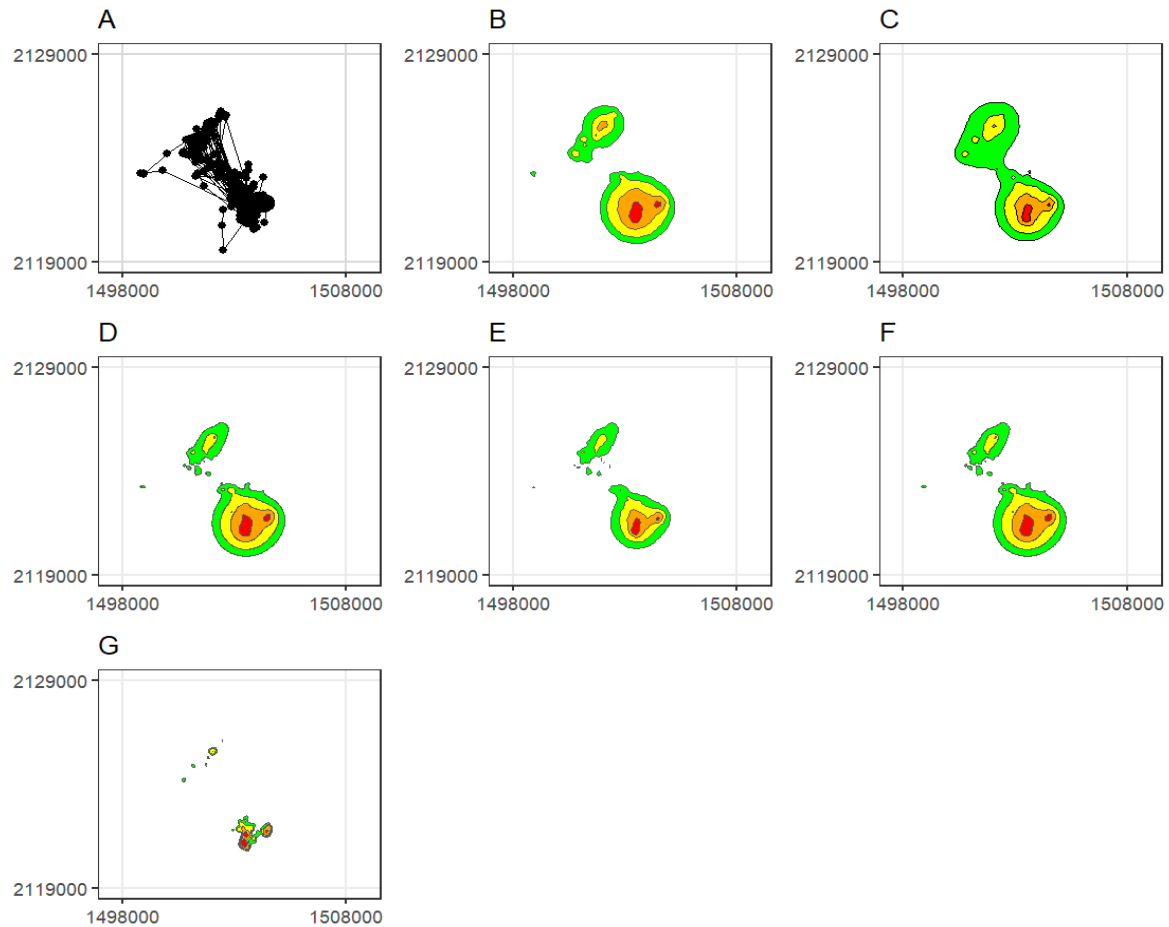


Figure 2.5 A) Breeding season GPS locations for AMCR007 in Pennsylvania, USA, 2024. Estimators of home range included: B) Brownian bridge movement model, C) dynamic Brownian bridge movement model, D) movement-based kernel density with null habitat, E) movement-based kernel density estimator with 4 land cover categories (water, developed, forest, open), F) movement-based kernel density with elevation, G) kernel density estimator with plug-in bandwidth selection. Isopleths are 50% (red), 80% (orange), 90% (yellow), and 95% (green).

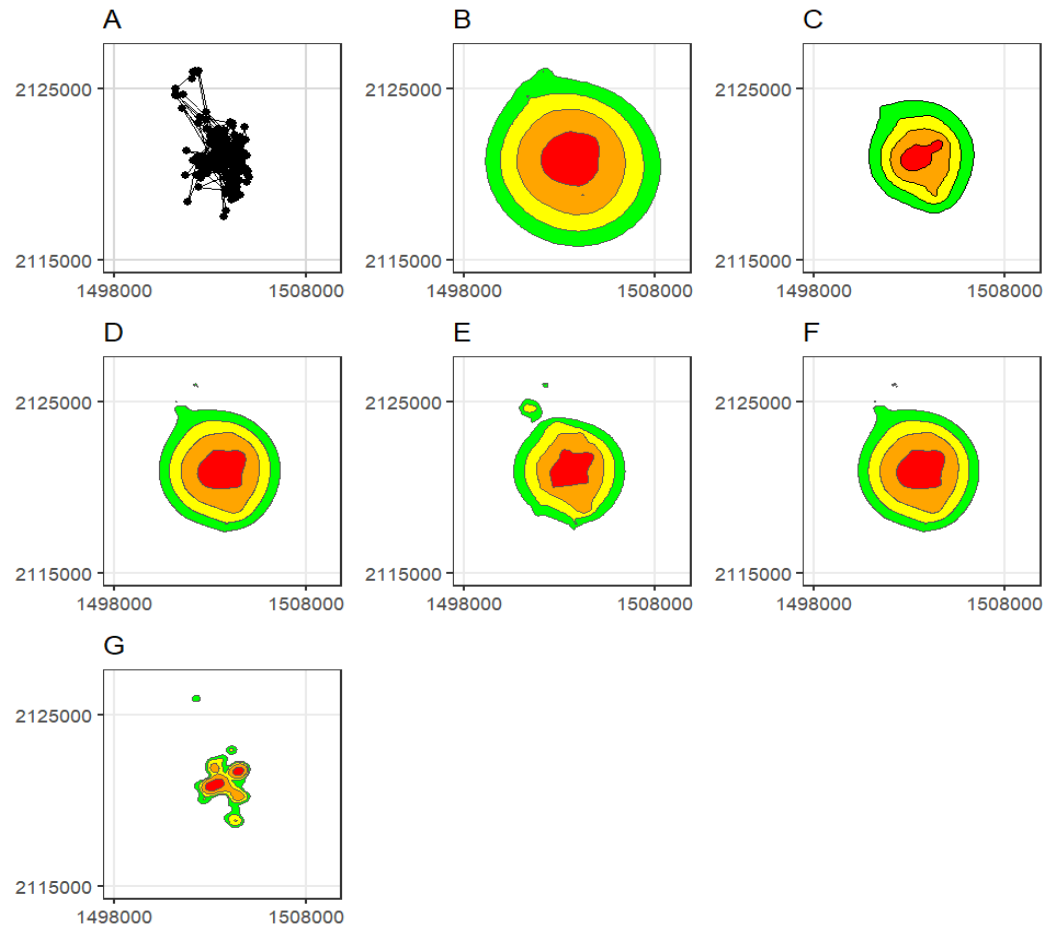


Figure 2.6 A) All season combined GPS locations for AMCR007 in Pennsylvania, USA, 2023-2024. Estimators of home range included: B) Brownian bridge movement model, C) dynamic Brownian bridge movement model, D) movement-based kernel density with null habitat, E) movement-based kernel density estimator with 4 land cover categories (water, developed, forest, open), F) movement-based kernel density with elevation, G) kernel density estimator with plug-in bandwidth selection. Isopleths are 50% (red), 80% (orange), 90% (yellow), and 95% (green).

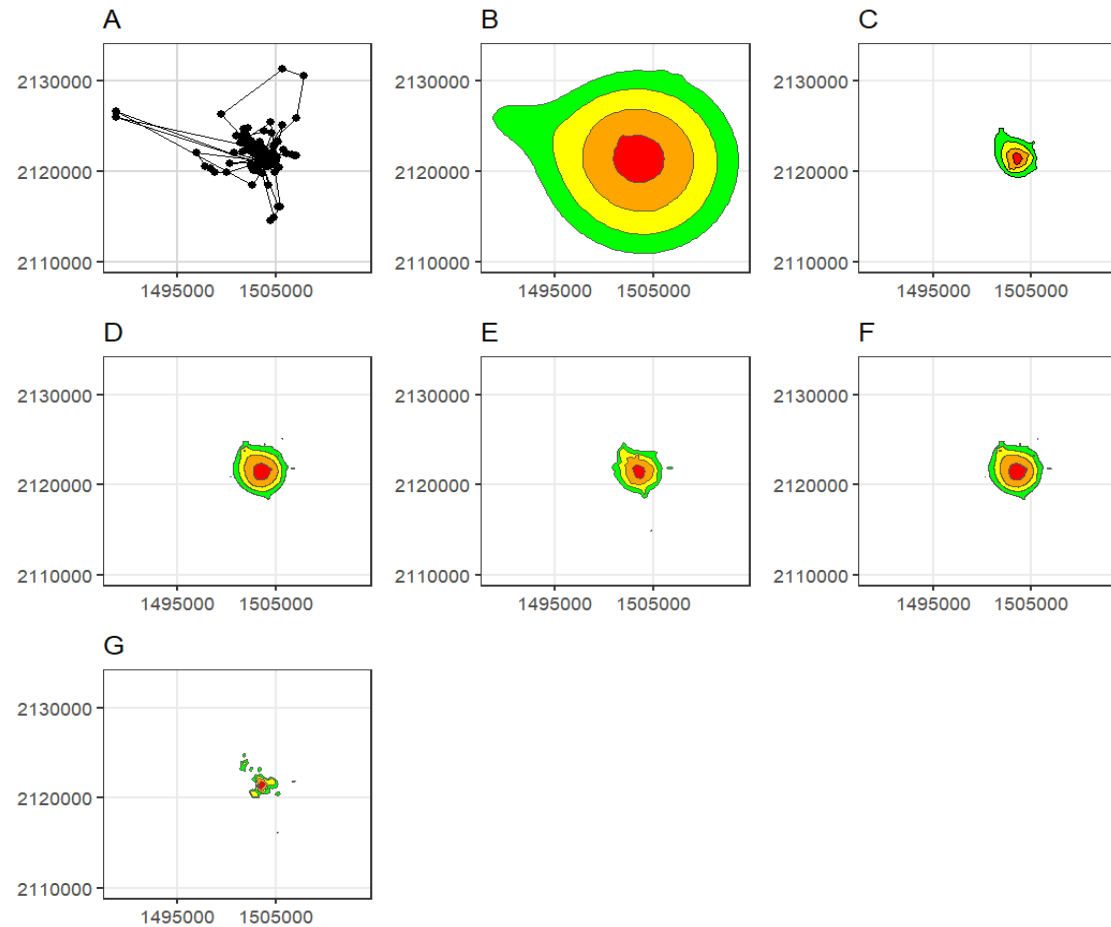


Figure 2.7 A) Nonbreeding season GPS locations for AMCR011 in Pennsylvania, USA, 2023-2024. Estimators of home range included: B) Brownian bridge movement model, C) dynamic Brownian bridge movement model, D) movement-based kernel density with null habitat, E) movement-based kernel density estimator with 4 land cover categories (water, developed, forest, open), F) movement-based kernel density with elevation, G) kernel density estimator with plug-in bandwidth selection. Isopleths are 50% (red), 80% (orange), 90% (yellow), and 95% (green).

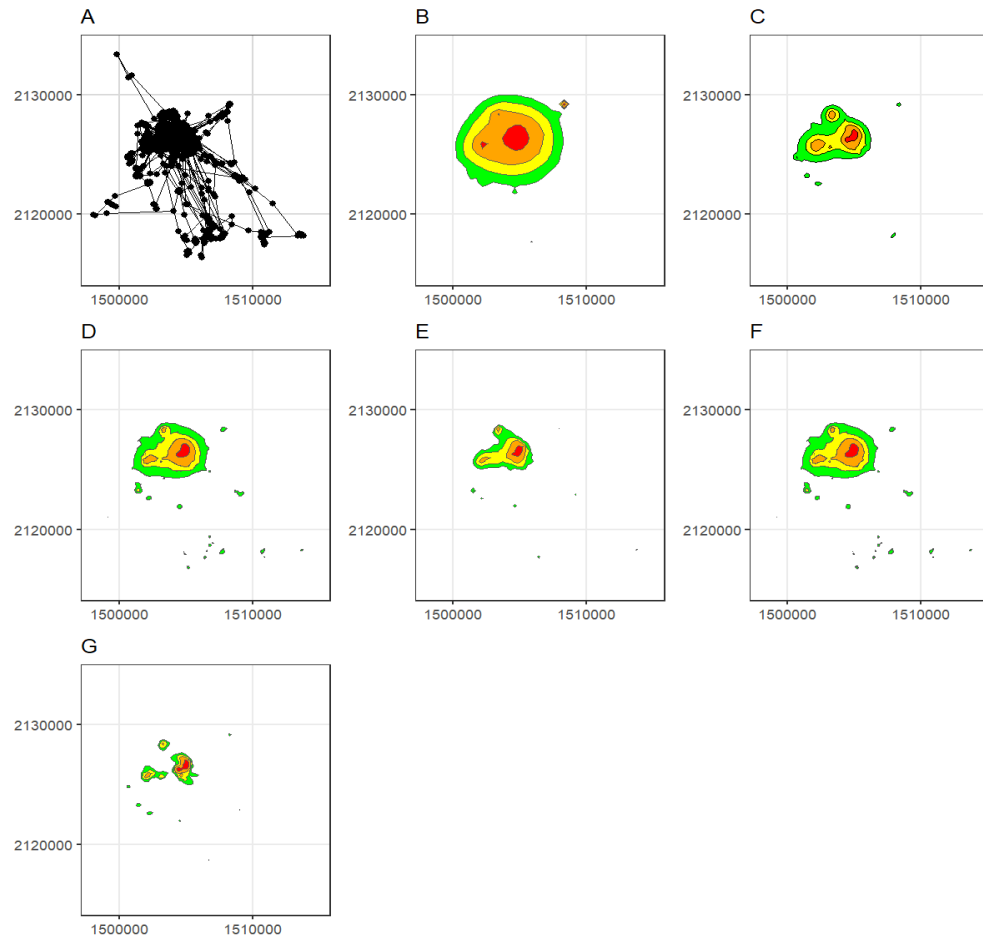


Figure 2.8 A) Breeding season GPS locations for AMCR011 in Pennsylvania, USA, 2024. Estimators of home range included: B) Brownian bridge movement model, C) dynamic Brownian bridge movement model, D) movement-based kernel density with null habitat, E) movement-based kernel density estimator with 4 land cover categories (water, developed, forest, open), F) movement-based kernel density with elevation, G) kernel density estimator with plug-in bandwidth selection. Isopleths are 50% (red), 80% (orange), 90% (yellow), and 95% (green).

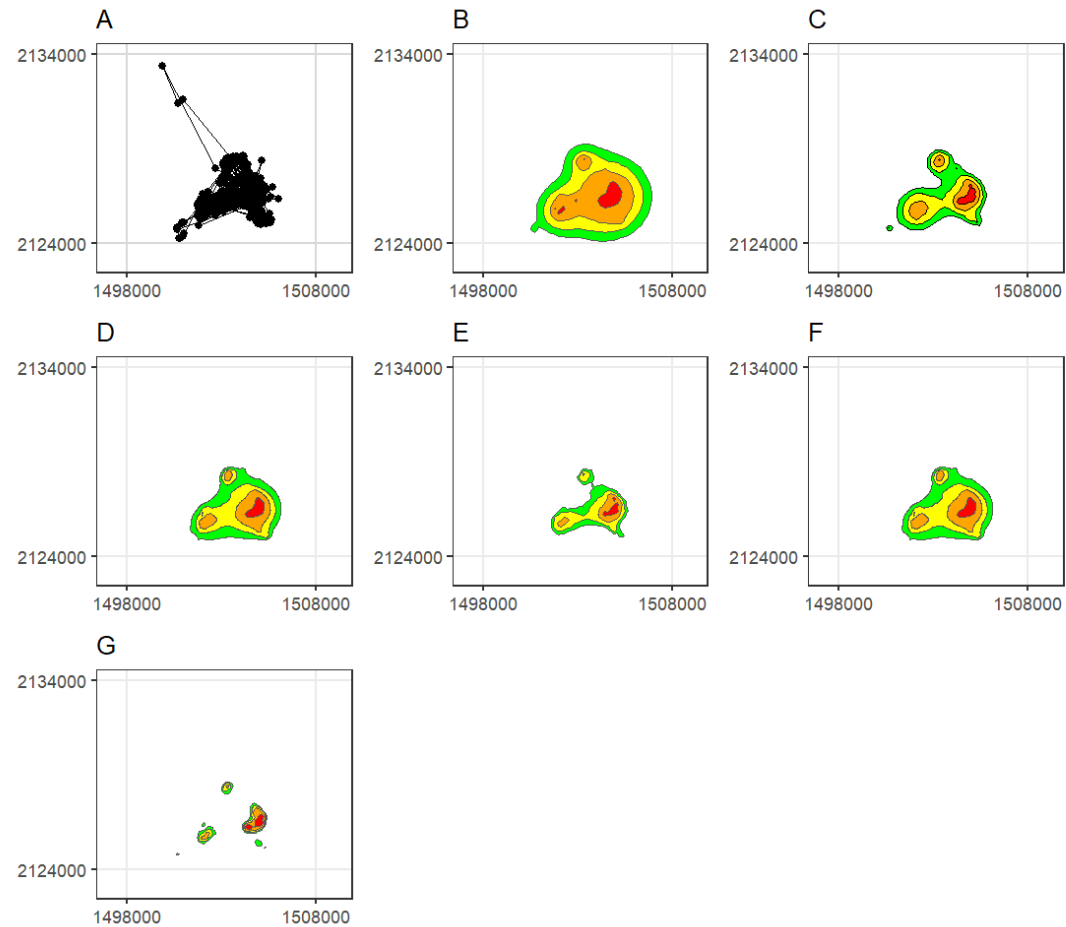


Figure 2.9 A) All seasons combined GPS locations for AMCR011 in Pennsylvania, USA, 2023-2024. Estimators of home range included: B) Brownian bridge movement model, C) dynamic Brownian bridge movement model, D) movement-based kernel density with null habitat, E) movement-based kernel density estimator with 4 land cover categories (water, developed, forest, open), F) movement-based kernel density with elevation, G) kernel density estimator with plug-in bandwidth selection. Isopleths are 50% (red), 80% (orange), 90% (yellow), and 95% (green).

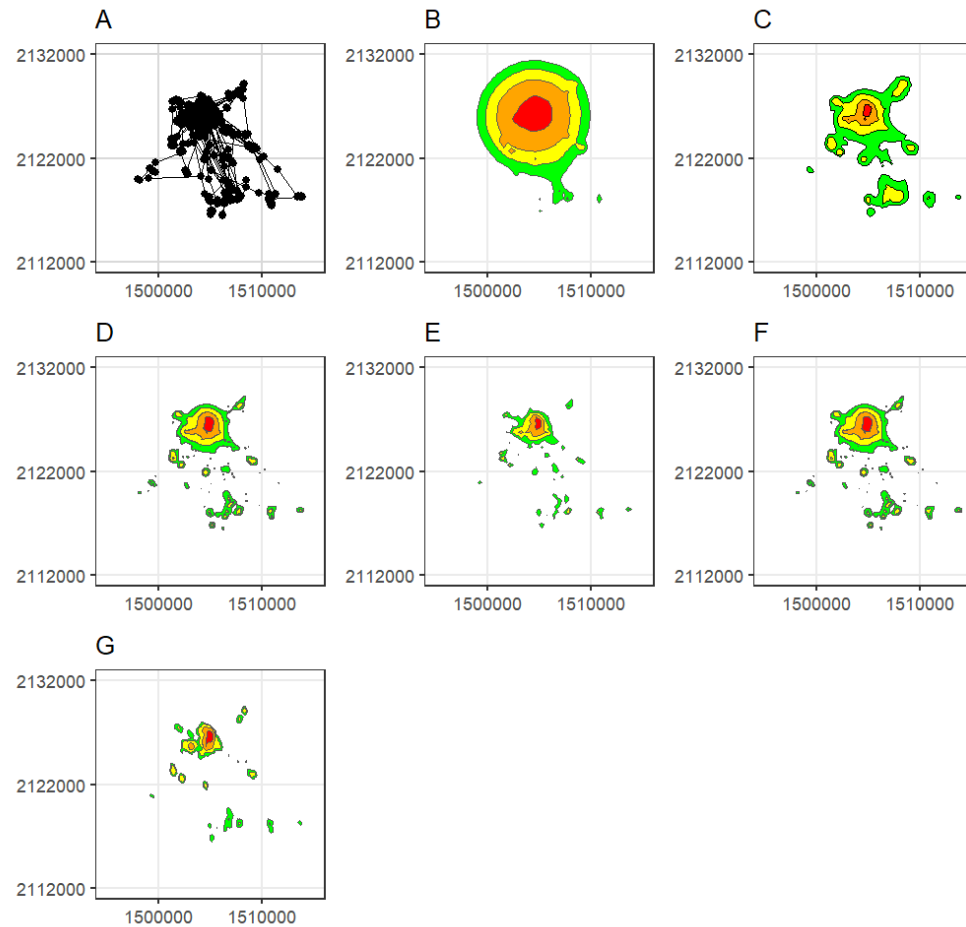


Figure 2.10 A) Breeding season GPS locations for AMCR012 in Pennsylvania, USA, 2024. Estimators of home range included: B) Brownian bridge movement model, C) dynamic Brownian bridge movement model, D) movement-based kernel density with null habitat, E) movement-based kernel density estimator with 4 land cover categories (water, developed, forest, open), F) movement-based kernel density with elevation, G) kernel density estimator with plug-in bandwidth selection. Isopleths are 50% (red), 80% (orange), 90% (yellow), and 95% (green).

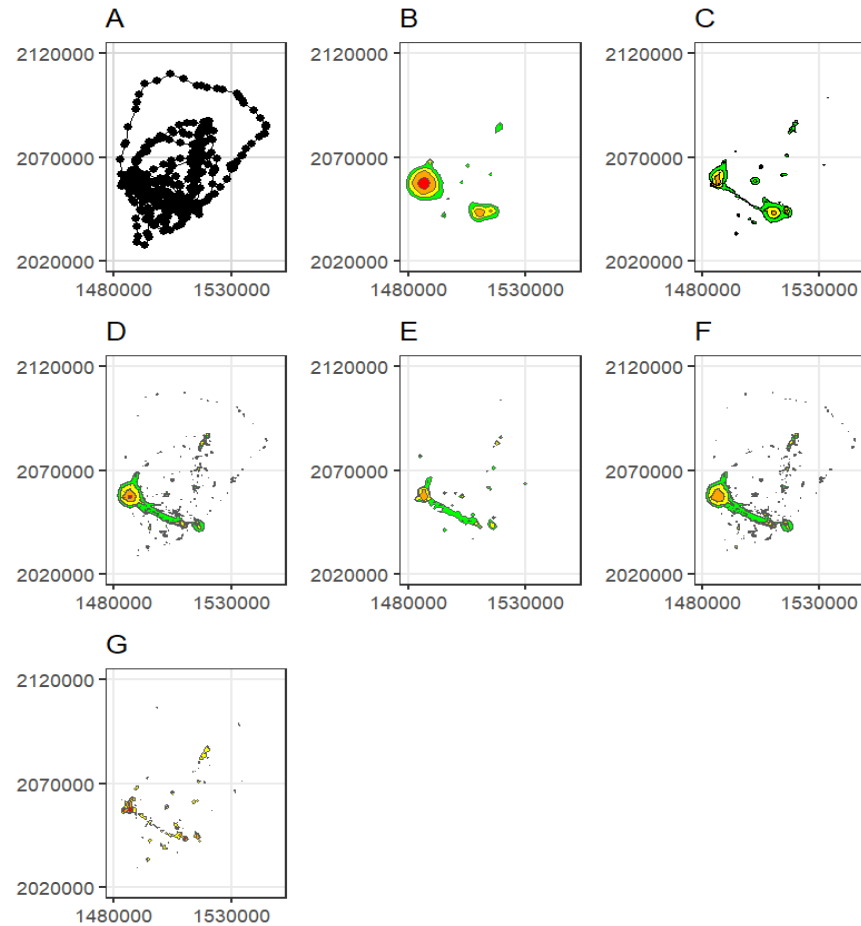


Figure 2.11 A) Breeding season GPS locations for AMCR013 in Pennsylvania, USA, 2024. Estimators of home range included: B) Brownian bridge movement model, C) dynamic Brownian bridge movement model, D) movement-based kernel density with null habitat, E) movement-based kernel density estimator with 4 land cover categories (water, developed, forest, open), F) movement-based kernel density with elevation, G) kernel density estimator with plug-in bandwidth selection. Isopleths are 50% (red), 80% (orange), 90% (yellow), and 95% (green).

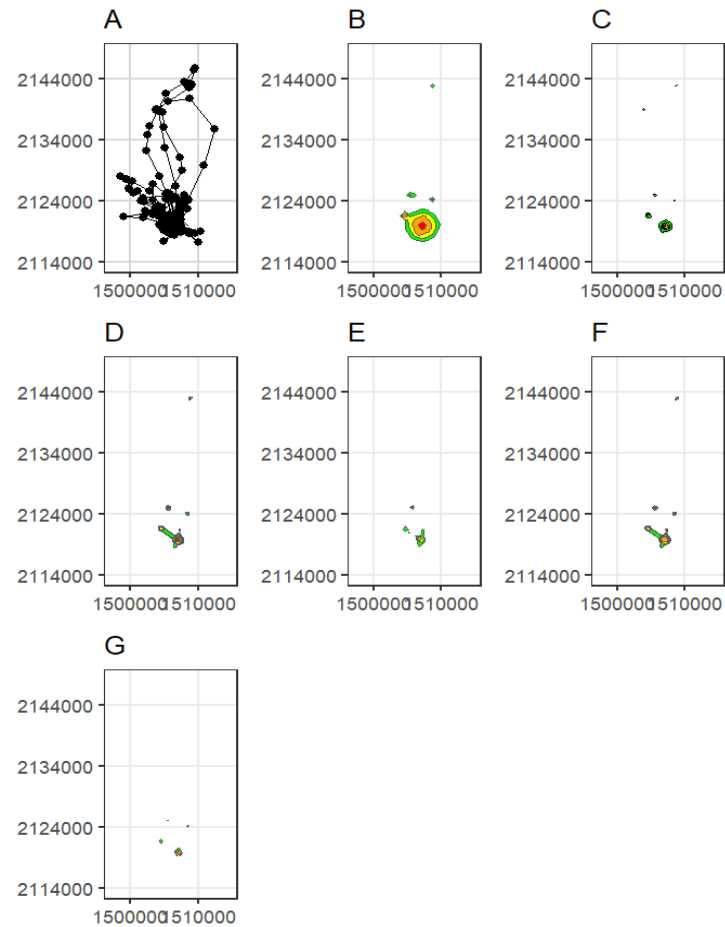


Figure 2.12 A) Breeding season GPS locations for AMCR014 in Pennsylvania, USA, 2024. Estimators of home range included: B) Brownian bridge movement model, C) dynamic Brownian bridge movement model, D) movement-based kernel density with null habitat, E) movement-based kernel density estimator with 4 land cover categories (water, developed, forest, open), F) movement-based kernel density with elevation, G) kernel density estimator with plug-in bandwidth selection. Isopleths are 50% (red), 80% (orange), 90% (yellow), and 95% (green).

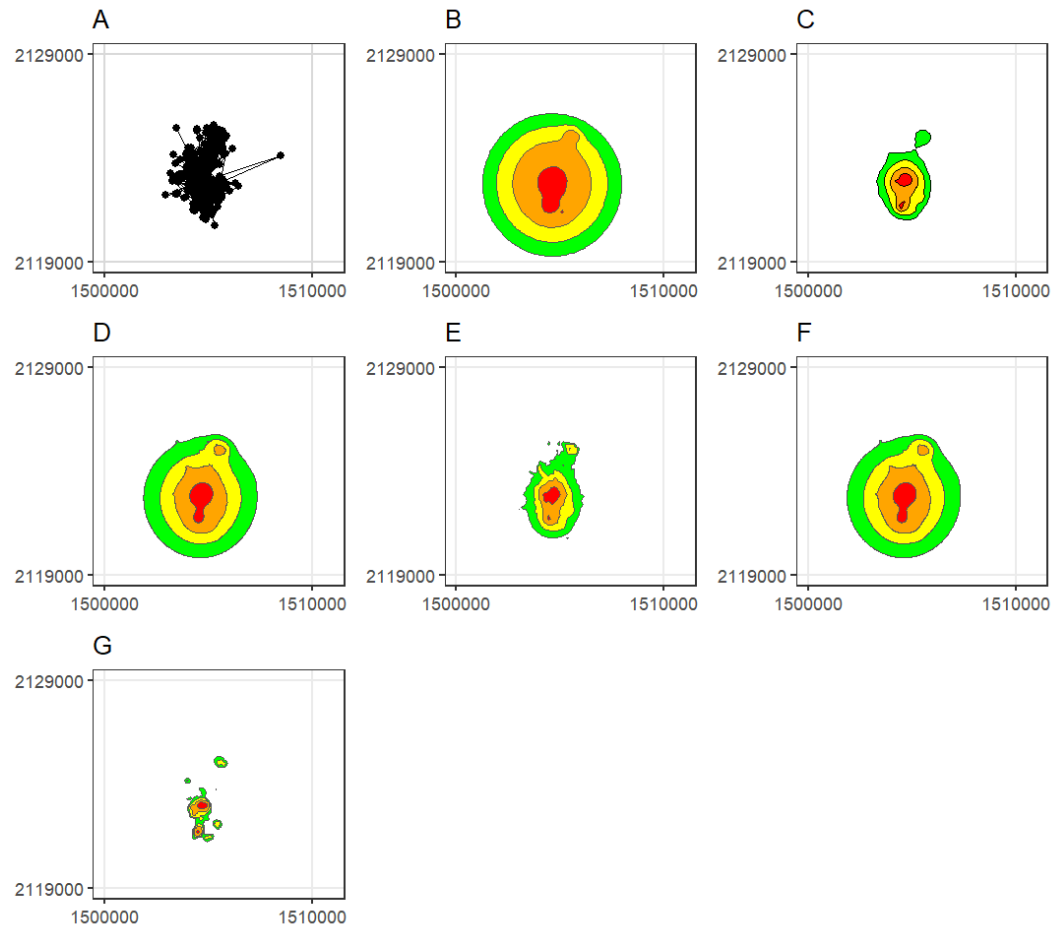
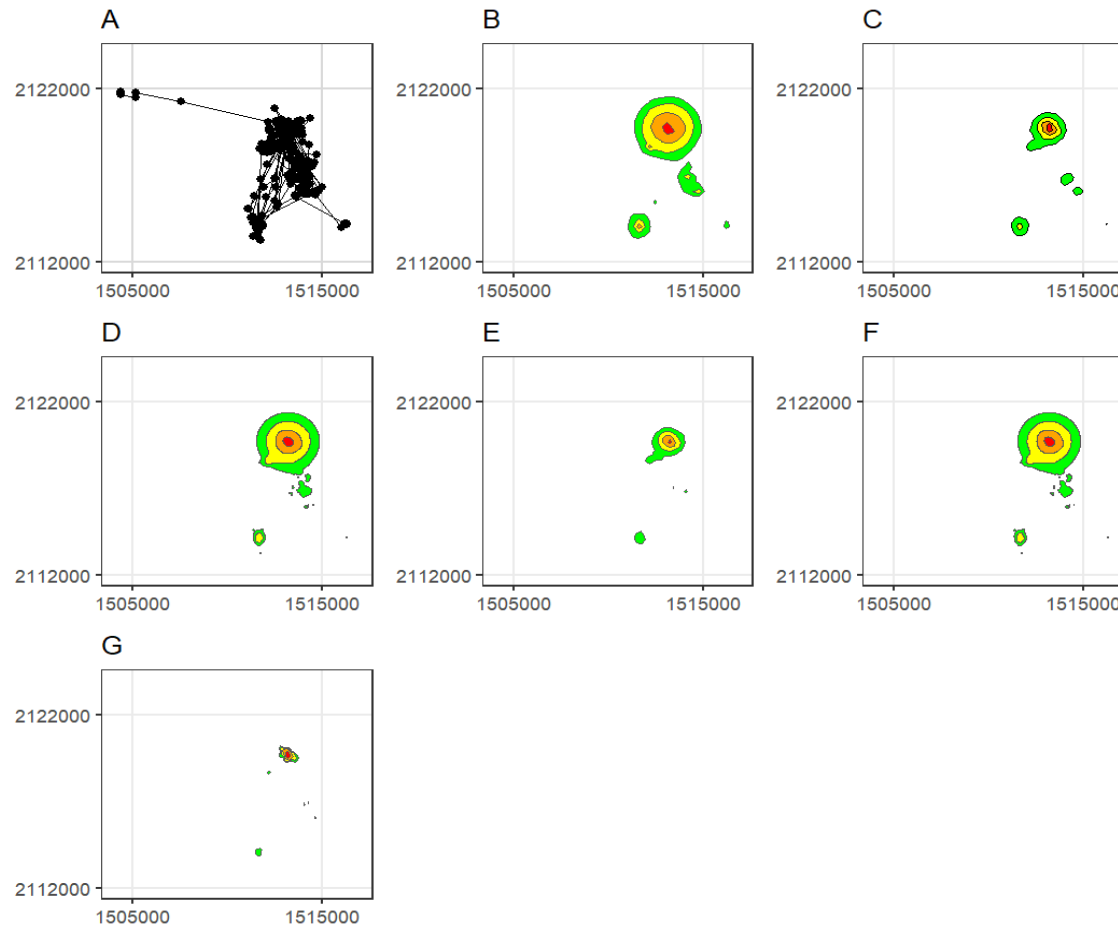


Figure 2.13 A) Breeding season GPS locations for AMCR015 in Pennsylvania, USA, 2024. Estimators of home range presented include: B) Brownian bridge movement model, C) dynamic Brownian bridge movement model, D) movement-based kernel density with null habitat, E) movement-based kernel density estimator with 4 land cover categories (water, developed, forest, open), F) movement-based kernel density with elevation, G) kernel density estimator with plug-in bandwidth selection. Isopleths are 50% (red), 80% (orange), 90% (yellow), and 95% (green).



Supplemental table 1. Comprehensive list of integrated step selection function models run for each individual and season.

Model elements
forest+waste+step length
forest+waste+elevation+step length
forest+risk+step length
forest+risk+elevation+step length
forest+roads+step length
forest+roads+elevation+step length
forest+h_pop+step length
forest+h_pop+elevation+step length
water+waste+step length
water+waste+elevation+step length
water+risk+step length
water+risk+elevation+step length
water+roads+step length
water+roads+elevation+step length
water+h_pop+step length
water+h_pop+elevation+step length
open+waste+step length
open+waste+elevation+step length
open+risk+step length
open+risk+elevation+step length
open+roads+step length
open+roads+elevation+step length
open+h_pop+step length
open+h_pop+elevation+step length
